

# An Introduction to Data Assimilation and Predictability in Geomagnetism

Alexandre Fournier · Gauthier Hulot ·  
Dominique Jault · Weijia Kuang · Andrew Tangborn ·  
Nicolas Gillet · Elisabeth Canet · Julien Aubert ·  
Florian Lhuillier

Received: 14 January 2010 / Accepted: 18 June 2010  
© Springer Science+Business Media B.V. 2010

**Abstract** Data assimilation in geomagnetism designates the set of inverse methods for geomagnetic data analysis which rely on an underlying prognostic numerical model of core dynamics. Within that framework, the time-dependency of the magnetohydrodynamic state of the core need no longer be parameterized: The model trajectory (and the secular variation it generates at the surface of the Earth) is controlled by the initial condition, and possibly some other static control parameters. The primary goal of geomagnetic data assimilation is then to combine in an optimal fashion the information contained in the database of geomagnetic observations and in the dynamical model, by adjusting the model trajectory in order to provide an adequate fit to the data.

---

A. Fournier (✉) · G. Hulot  
Géomagnétisme, Institut de Physique du Globe de Paris, Université Paris Diderot, CNRS,  
4 place Jussieu, 75252 Paris cedex 5, France  
e-mail: [fournier@ipgp.fr](mailto:fournier@ipgp.fr)

D. Jault · N. Gillet · E. Canet  
Laboratoire de Géophysique Interne et Tectonophysique, CNRS, Université Joseph-Fourier, Grenoble,  
France

W. Kuang  
Planetary Geodynamics Laboratory, Goddard Space Flight Center, Greenbelt, MD, USA

A. Tangborn  
Joint Center for Earth Systems Technology, University of Maryland Baltimore County, Baltimore, MD,  
USA

E. Canet  
Institut für Geophysik, ETH Zürich, Zürich, Switzerland

J. Aubert  
Dynamique des Fluides Géologiques, Institut de Physique du Globe de Paris, Paris, France

F. Lhuillier  
Géomagnétisme & Dynamique des Fluides Géologiques, Institut de Physique du Globe de Paris, Paris,  
France

The recent developments in that emerging field of research are motivated mostly by the increase in data quality and quantity during the last decade, owing to the ongoing era of magnetic observation of the Earth from space, and by the concurrent progress in the numerical description of core dynamics.

In this article we review briefly the current status of our knowledge of core dynamics, and elaborate on the reasons which motivate geomagnetic data assimilation studies, most notably (a) the prospect to propagate the current quality of data backward in time to construct dynamically consistent historical core field and flow models, (b) the possibility to improve the forecast of the secular variation, and (c) on a more fundamental level, the will to identify unambiguously the physical mechanisms governing the secular variation. We then present the fundamentals of data assimilation (in its sequential and variational forms) and summarize the observations at hand for data assimilation practice. We present next two approaches to geomagnetic data assimilation: The first relies on a three-dimensional model of the geodynamo, and the second on a quasi-geostrophic approximation. We also provide an estimate of the limit of the predictability of the geomagnetic secular variation based upon a suite of three-dimensional dynamo models. We finish by discussing possible directions for future research, in particular the assimilation of laboratory observations of liquid metal analogs of Earth's core.

**Keywords** Geomagnetic secular variation · Dynamo: theories and simulations · Earth's core dynamics · Inverse theory · Data assimilation · Satellite magnetics · Predictability

## 1 Introduction

### 1.1 Inference on Core Dynamics from Geomagnetic Observations

We begin with a brief overview of the current status of our knowledge of core dynamics, as deduced from the record of the geomagnetic secular variation. In addition to the various references listed in this section, the interested reader will find a complete account of the theoretical and observational foundations of that knowledge in the reviews by Jackson and Finlay (2007) and Finlay et al. (2010).

Inferences on sub-annual to decadal core dynamics are usually made by assuming that the geomagnetic secular variation at the core-mantle boundary (CMB), as described by the rate-of-change of the radial component of the magnetic induction  $\partial_t B_r$ , is caused by diffusionless advection by the fluid flow  $\mathbf{u}_h$ :

$$\partial_t B_r = -\nabla_h \cdot (\mathbf{u}_h B_r), \quad (1)$$

in which  $\nabla_h \cdot$  is the horizontal divergence operator. This so-called frozen-flux hypothesis was originally proposed by Roberts and Scott (1965); it is of central importance for finding estimates of the flow at the top of the core responsible for the observed secular variation. As such, the problem is non-unique (Backus 1968). Consequently, further assumptions on  $\mathbf{u}_h$  are needed; those are reviewed in detail and discussed by Holme (2007) and Finlay et al. (2010). In addition, the product of the inversion is often regularized: Intermediate—to small-scale features are damped in order to produce a flow of moderate spatial complexity. In the past thirty years, tens of studies based on different approaches have arguably produced a common, large-scale picture of  $\mathbf{u}_h$  for recent epochs (Holme 2007): it consists in a strong westward flow under the Atlantic ocean, a flow usually weaker under the Pacific hemisphere, and it exhibits large-scale vortices under South Africa and North America, the root

mean square (rms) flow speed being on the order of 15 km/y. Further inspection of various core flow models produced under different working hypotheses reveals features which are far less consensual, and hypotheses-dependent (Holme 2007, and references therein). The large-scale, consensual picture described above evolves slowly over time, as do the large-scale features of the magnetic field (e.g. Hulot and Le Mouél 1994).<sup>1</sup> This can be observed by considering either snapshots of  $\mathbf{u}_h$  at different epochs (e.g. Hulot et al. 1993), or parameterized, time-dependent core flow models, as computed by Jackson (1997) (recall that time is a parameter, and not a variable, within the kinematic framework we have discussed so far).

In an attempt to relate the dynamics inferred at the top of the core with its deeper origin, the axisymmetric component of time-dependent core surface motions can in turn be interpreted as the signature of torsional oscillations occurring inside the core (Braginsky 1970). The subject of torsional oscillations is reviewed by Finlay et al. (2010). Trying to fit the secular variation (or to explain time-dependent core flow) using that class of wavy motions is of great interest, since it provides in particular constraints on the strength of the cylindrical radial magnetic induction inside the core,  $B_s$ . For a recent effort in that direction, consult Buffett et al. (2009).

The path from geomagnetic observations to the description of core dynamics has thus so far mostly consisted in a two-stage, sequential process: First,  $B_r$  and  $\partial_t B_r$  are estimated at the CMB by downward-continuing surface measurements, using some regularization. Second, the surface flow underneath the CMB is estimated from (1), by imposing one (or several) constraints on the flow, and inevitably some damping. However and regardless of the lack of consistency of that strategy, it now appears that our ability to learn more about core dynamics following this path has almost reached a plateau, even though the quality and density of the recent data keep on improving. This is because spatial resolution errors<sup>2</sup> (the large-scale secular variation due to the interaction of the concealed, small-scale field, with the large-scale flow) now dominate observational errors in the error budget of core flow inversions (Eymin and Hulot 2005).

More recently, sophisticated strategies, such as ensemble approaches, have been used to describe statistically the corresponding unresolved component of the secular variation (Gillet et al. 2009). Modeling strategies bypassing the above two-stage, sequential approach have also been designed to simultaneously invert for the field and the flow at the top of the core (Lesur et al. 2010), in philosophical line with an earlier work by Waddington et al. (1995). Lesur et al. (2010) implement the frozen-flux constraint (equation (1)) in their inversion, thereby introducing a dynamically consistent relationship between  $B_r$  and  $\mathbf{u}_h$  at the top of the core.

These two recent and innovative approaches very much point the way forward to a better understanding and description of core dynamics, by incorporating dynamical constraints (as imposed by the equations governing the secular variation of the geomagnetic field) in the inversion process, and taking spatial resolution errors into account in the most sensible way. Such preoccupations are not limited to the study of the geomagnetic secular variation: During the past decades, they have also been central in the fields of atmospheric dynamics and physical oceanography, and at the heart of the development of data assimilation strategies.

<sup>1</sup>Note, though, that recent field models based on satellite data indicate a reorganization time for the large-scale structures of the secular variation  $\partial_t B_r$  itself on the order of 20 y (Olsen et al. 2009).

<sup>2</sup>Also called “errors of representativeness” in the data assimilation literature (e.g. Lorenç 1986; Kalnay 2003; Brasseur 2006).

The terminology “data assimilation” was coined in meteorology to label the set of time-dependent, inverse techniques used for improving the forecast of the state of the atmosphere. In his authoritative article, Talagrand (1997) defines the assimilation of meteorological or oceanographical observations as the process through which all the available information is used in order to estimate as accurately as possible the state of the atmospheric or oceanic flow. Here we complement that definition by explicitly adding that the determination of the associated uncertainty is also desirable.

## 1.2 A Historical Perspective on Atmospheric Data Assimilation and Numerical Weather Prediction

Precisely because atmospheric data assimilation is so much ahead of geomagnetic data assimilation, it is worth providing the reader first with a brief historical perspective on that area of research (and the related issue of numerical weather prediction). The standards defined by this more mature field will naturally lead us to further argue for the need to develop geomagnetic data assimilation systems.

Data assimilation was initially developed as a means to initialize atmospheric models for use in Numerical Weather Prediction (NWP). Early efforts to predict atmospheric motion through calculation began even before the advent of digital computers. Richardson (1922) developed the first numerical weather prediction system, using a room full of human calculators, and was ultimately unsuccessful. Observations of the atmosphere were hand interpolated to a regular grid in order to initialize an early equations of motion and state system, taking 6 weeks to carry out a 6-hour forecast. The development of early computers led to an effort by Charney et al. (1950), which used numerical interpolation to fit observational data to a regular grid.

The general approach of interpolating a numerical forecast to observation location, calculating the difference between observation and forecast ( $O - F$ ) (termed the innovation) and interpolating back to the numerical grid, was first developed by Bergthorsson and Döös (1955). This difference was then used to correct the forecast as an initialization of the next segment of the model forecast. Statistical interpolation, a Bayesian approach for giving relative weights to the observations and forecast, was next introduced by Eliassen (1954) and Gandin (1963).

From this time forward the field of numerical weather prediction progressed rapidly, and still continues to do so: the 72-hour forecasts are now as successful (as measured by the average error in the determination of the horizontal pressure gradient over a given area) as the 36-hour forecasts were 10 or 20 years ago (Kalnay 2003). Kalnay (2003) attributes that continuous improvement to the conjunction of four factors:

- (F1) the increased power of supercomputers, allowing much finer numerical resolution and fewer approximations in the operational atmospheric models;
- (F2) the improved representation of small-scale physical processes (clouds, precipitation, turbulent transfers of heat, moisture, momentum, and radiation) within the models;
- (F3) the use of more accurate methods of data assimilation, which results in improved initial conditions for the model; and
- (F4) the increased availability of data, especially satellite and aircraft data over the oceans and the Southern hemisphere.

It is striking to see how those factors can equally well be listed as necessary conditions for progress to occur in the field of geomagnetic data analysis and its interpretation in terms of the underlying core dynamics.

### 1.3 Why Consider Geomagnetic Data Assimilation

It is quite tempting to wonder how the learning curve of atmospheric data assimilation carries over to the subject of geomagnetic data analysis. An intermediate learning curve would actually be that of ocean data assimilation (Ghil and Malanotte-Rizzoli 1991): the interested reader will find in the monograph edited by Chassignet and Verron (2006) an account of its evolution over the past fifteen years, in the wake of the launch of several satellite missions to monitor the state of the world ocean (the Global Ocean Observation System),<sup>3</sup> which led to the international Global Ocean Data Assimilation Experiment program.<sup>4</sup> In geomagnetism, alongside the recent increase in the quantity and quality of observations (factor F4 above, which is described succinctly in Sect. 3 below, and more substantially by Hulot et al. 2007 and Gillet et al. 2010b), there has been considerable improvement in our ability to model numerically the non-linear dynamics of the core since the groundbreaking work of Glatzmaier and Roberts (1995) (e.g. Christensen and Wicht 2007; Sakuraba and Roberts 2009). This improvement essentially follows on from the increase in computational power, and the development of codes able to capitalize on the parallel trend in high-performance computing (factor F1 above). Three-dimensional, convection-driven models of the geodynamo are of particular interest since they are now used to derive scaling laws for its average behavior. Key non-dimensional parameters controlling that behavior can be identified in a database of such models, and for instance used to evaluate, after appropriate extrapolation, the rms strength of the magnetic field inside the core, which is of order 2 mT according to Christensen and Aubert (2006) and Christensen et al. (2009). Despite that indisputable progress, questions remain concerning the applicability of such numerical tools to geomagnetic field modelling, depending on the time scale of interest. Practical numerical considerations make the value of some input diffusive control parameters too large (by several orders of magnitude) compared to what one would expect for the Earth. Part of the dynamics is thus certainly affected (damped) in such numerical simulations (that includes the torsional oscillations). Also, a good modelling of the secular variation on interannual time scales requires a proper separation of the time scales of the relevant physical phenomena, in line with what occurs in the core. These phenomena include inertial waves (which build geostrophy), various types of magnetohydrodynamic waves, advection, and Ohmic dissipation; the corresponding time scales are roughly of order 1 day, 10 yr, 100 yr, and 10,000 yr, respectively (e.g. Gubbins and Roberts 1987; Jault 2008; Finlay et al. 2010). Having those time scales in the right proportion is currently not easily achievable with three-dimensional dynamo models. Their ability to cope with that mismatch will be assessed through their success in analyzing and forecasting short-term geomagnetic changes (in light of the available observations).

Alternatively, one can be tempted to circumvent that overdiffusive behavior by simplifying the model of core dynamics, thereby reducing its dimensionality and making less diffusive simulations, with an appropriate separation of the relevant timescales, possible (at the expense of some physics lost along the way). An example is the quasi-geostrophic approach, which assumes that the flow is invariant along the direction of rotation of the Earth, and effectively considers a two-dimensional flow. The validity of that approach (depending on the time scale and the region under scrutiny) is addressed in Sect. 4.2. In what follows, we actually make a case for geomagnetic data assimilation as a way to test to which extent

---

<sup>3</sup>[www.ioc-goos.org](http://www.ioc-goos.org).

<sup>4</sup>[www.godae.org](http://www.godae.org).

a given model can be successful in explaining our indirect observations of core dynamics. Bearing in mind the recent evolution in the observation of the geomagnetic field and the modelling of core dynamics, we now list some of the questions which we would like to try and answer using geomagnetic data assimilation:

1. Can the physical mechanisms responsible for the geomagnetic secular variation be identified unambiguously in its record? As an example, are surface measurements the signature of effective material transport of  $B_r$  at the CMB, or the signature of hydromagnetic waves (Finlay and Jackson 2003)? Those two effects could very well be combined, and, despite the popularity of the frozen-flux approach, an ounce (or more) of diffusion might also be required (Gubbins 1996; Chulliat and Olsen 2010; Chulliat et al. 2010). Assimilation of geomagnetic measurements into models of core dynamics will first and foremost tell us something about the various models we resort to. As outlined above, a comprehensive model of core dynamics, able to represent all the physics occurring at all time and length scales, is not within reach. Compromises have to be made, and geomagnetic data assimilation appears as the natural framework within which to evaluate the robustness of those compromises, in the light of the data.
2. What is the predictive power of dynamical models of the geomagnetic field? That question is related to the problem of forecasting, a long-standing issue of interest in numerical weather prediction (see Sect. 1.2 above).
3. To which extent is it possible to retro-propagate the current quality of data for the purpose of core field modelling? That question is related to the issue of hindcasting, or reanalysis. Here a reference is the work done on the reanalysis of the state of the atmosphere over the time period 1957–1996, that is supposed to be free of artifacts resulting from changes in the assimilation/analysis techniques used initially in that time interval (Kalnay et al. 1996). This reanalysis has allowed one to recompute more accurately the atmospheric angular momentum over that same time window, and its related contribution to the length-of-day (LOD) time series (Gross et al. 2004).

Regarding that last point, the interest for data assimilation lies in its versatility regarding the type of measurements it can use to obtain some insights on the state of the system under study. Any measurement (even remotely related to the state of system) can be used. The quality and quantity of information contained in those measurements can also vary widely with time, which makes data assimilation particularly well-suited for geomagnetic purposes.

Finally, specific to the core problem is the attractive possibility offered by the joint use of models and observations to probe (indirectly) the deeper dynamics of the core by analyzing its magnetic surficial signature at the core-mantle boundary.

The remainder of this article aims at discussing the possibility of addressing the questions listed above in a foreseeable future with the help of data assimilation. It is organized as follows: The methodological foundations of data assimilation are first presented in Sect. 2. Section 3 summarizes next the observations at hand for geomagnetic data assimilation practice. Section 4 reviews recent studies devoted to the feasibility and application of data assimilation techniques for the purpose of geomagnetic data analysis. Two options have been followed so far:

- One option relies on three-dimensional numerical models of the geodynamo, and is illustrated in Sect. 4.1. Three-dimensional models of the geodynamo have actually also been used to try and estimate the limit of predictability of the secular variation, an account of which is provided in Sect. 4.3.
- Another option is based upon quasi-geostrophic models of the secular variation, and is the subject of Sect. 4.2.

Section 5 concludes this review by providing a tentative summary and by pointing out possible directions for future research.

## 2 Fundamentals of Data Assimilation

In this section we aim at describing the fundamentals of data assimilation, in its sequential and variational formulations, without providing any proof of the underlying mathematical results. The interested reader will find a much more rigorous and complete treatment of the subject in the recent treatises by Bennett (2002), Kalnay (2003), Wunsch (2006), and Evensen (2009). We will resort as much as possible to the set of notations recommended by Ide et al. (1997); our notations are summarized in Table 1.

### 2.1 Basic Ingredients

The goal of geomagnetic data assimilation is to solve the time-dependent inverse problem of estimating the state of the core  $\mathbf{x}$ , with time appearing as an explicit variable. We have at

**Table 1** Data assimilation notations used in this paper, which follow for the most part the recommendations made by Ide et al. (1997). With the exception of the objective function  $J$ , the quantities listed in this table are time-dependent, and appear in the text with an index  $i$  referring to the discrete time  $t_i$  at which they come into play

Symbol	Meaning
$\mathbf{x}$	the state vector of the core
$L_{\mathbf{x}}$	size of the state vector
$\mathbf{x}^t$	the true state
$M$	the forward model of core dynamics
$\eta$	the model error
$\mathbf{Q}$	the model error covariance matrix
$\mathbf{x}^f$	the forecast
$\epsilon^f$	the forecast error
$\mathbf{P}^f$	the forecast error covariance matrix
$\mathbf{x}^a$	the analysis
$\epsilon^a$	the analysis error
$\mathbf{P}^a$	the analysis error covariance matrix
$\mathbf{x}^b$	the background state
$\mathbf{P}^b$	the background error covariance matrix
$H$	the observation operator
$H' \equiv \mathbf{H}$	the linearized observation operator
$\mathbf{y}^o$	the observations
$L_{\mathbf{y}^o}$	size of the observation vector
$\epsilon^o$	the observational error
$\mathbf{R}$	the observational error covariance matrix
$K$	the Kalman gain
$J$	the objective function
$M' \equiv \mathbf{M}$	the tangent linear model
$M'^T \equiv \mathbf{M}^T$	the adjoint model
$\mathbf{d}$	the innovation
$\mathbf{r}$	the residual
$\mathbf{a}$	the adjoint field

our disposal a database of observations of the core and a numerical model of its dynamics. Before proceeding with technicalities, we quote Wunsch (2006): "...almost all methods in actual use are, beneath the mathematical disguises, nothing but versions of least-square fitting of models to data, but reorganized so as to increase the efficiency of solution, or to minimize storage requirements, or to accommodate continuing data streams."

In the remainder of this section, we shall operate in a discrete world. Assume we have a prognostic, possibly non-linear, numerical model  $M$  which describes the dynamical evolution of the core state at any discrete time  $t_i, i \in \{0, \dots, n\}$ . If  $\Delta t$  denotes the time-step size, the width of the time window considered here is  $T = t_n - t_0 = n\Delta t$ , the initial (final) time being  $t_0$  ( $t_n$ ). In formal assimilation parlance, this is written as

$$\mathbf{x}_{i+1} = M_{i,i+1} [\mathbf{x}_i], \quad (2)$$

in which  $\mathbf{x}_i$  is a column vector (of size  $L_{\mathbf{x}_i}$ , say), describing the state of the core at discrete time  $t_i$ . If  $M$  relies for instance on a grid-based discretization of the equations governing the geomagnetic secular variation, then the state vector  $\mathbf{x}$  contains the values of all the corresponding field variables at every grid point. The secular variation equations could involve terms with a known, explicit time dependence, hence the dependence of  $M$  on time in (2). In the remainder of this paper, we shall omit the model operator time indices for the sake of clarity, unless necessary. Within this framework, the modeled secular variation is controlled by the initial state of the core,  $\mathbf{x}_0$ , and possibly some other, static, input parameters. The model operator is imperfect: Even if we knew the true state of the core  $\mathbf{x}_i^t$  at discrete time  $t_i$ , the action of the model would introduce a simulation error  $\boldsymbol{\eta}_{i+1}$  at time  $t_{i+1}$ , defined as

$$\boldsymbol{\eta}_{i+1} = M [\mathbf{x}_i^t] - \mathbf{x}_{i+1}^t. \quad (3)$$

In the following, the statistical distribution of that error is assumed to be Gaussian and centered, and we denote the simulation error covariance matrix with  $\mathbf{Q}_i$ .

Assume now that we have partial and imperfect knowledge of the true dynamical state of the core  $\mathbf{x}^t$  through databases of observations  $\mathbf{y}^o$  collected at discrete locations in space and time. This formally writes

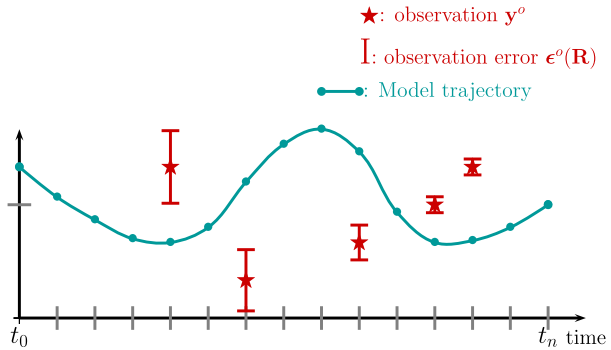
$$\mathbf{y}_i^o = H_i [\mathbf{x}_i^t] + \boldsymbol{\epsilon}_i^o, \quad (4)$$

in which  $\mathbf{y}_i^o$  is a column vector of size  $L_{\mathbf{y}_i^o}$ , and  $H_i$  and  $\boldsymbol{\epsilon}_i^o$  are the (possibly time-dependent) discrete observation operator and error, respectively. Modern geomagnetic observations consist of (scalar or vector) measurements of the magnetic field, possibly supplemented by annual to decadal time series of the length-of-day, since these are related to the angular momentum of the core (see Sect. 3). The observation operator is assumed time-dependent: In the context of geomagnetic data assimilation, we can safely anticipate that its dimension will increase dramatically when entering the recent satellite era (1999–present). However,  $H_i$  will inevitably connect  $\mathbf{x}$  with a space of lower dimensionality than the state space ( $L_{\mathbf{y}_i^o} < L_{\mathbf{x}_i}$ , see Table 2). The observational error  $\boldsymbol{\epsilon}_i^o$  is time-dependent as well. We will assume in the following that it has zero mean and we will denote its covariance matrix at discrete time  $t_i$  by  $\mathbf{R}_i$ . For simplicity and unless otherwise stated, we will also assume that the observation operator is linear, namely that  $H = H' \equiv \mathbf{H}$  according to the notations of Table 1.

As illustrated in Fig. 1, we may have a first guess of the model trajectory over the time interval of interest, and some observations (along with their error statistics) available along the way. Our task is to make the best (optimal) use of those available measurements in order to correct the initial trajectory. This can be achieved following either of two strategies, referred to as sequential or variational data assimilation, which we will now introduce.



**Fig. 1** Assimilation starts with an unconstrained model trajectory over the time window of interest. It aims at correcting this initial model trajectory in order to provide an optimal fit to the available observations (*the stars*), given their *error bars*. In this figure (and also in Figs. 3 and 4), it is assumed for pedagogical simplicity that the state vector and the observation vector belong to the same one-dimensional space



## 2.2 Methodology: Two Classes of Implementation

### 2.2.1 Sequential Assimilation

Sequential assimilation is rooted in estimation theory and its two-stage principle is the following: Starting from a previously analyzed core state, we first forecast the evolution of that state, and then correct it (i.e. perform an analysis) as soon as an observation is available. For the sake of simplicity, we shall defer the discussion of the non-linear case and consider for now that  $M$  is linear.

1. The forecast: In mathematical terms, the forecast at time  $t_{i+1}$ ,  $\mathbf{x}_{i+1}^f$ , is obtained by time-stepping the model, starting from the a priori, analyzed state  $\mathbf{x}_i^a$ <sup>5</sup> at time  $t_i$ :

$$\mathbf{x}_{i+1}^f = M\mathbf{x}_i^a. \tag{5}$$

The forecast error writes accordingly

$$\epsilon_{i+1}^f = \mathbf{x}_{i+1}^f - \mathbf{x}_{i+1}^t = M(\mathbf{x}_i^a - \mathbf{x}_i^t) + \eta_{i+1}, \tag{6}$$

which shows that it has two components (see Fig. 2):

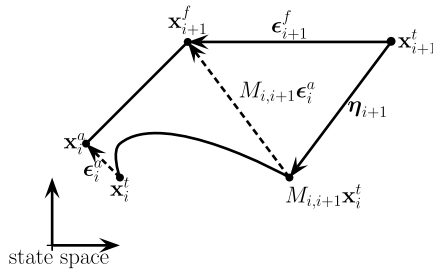
- The propagated error in the a priori, analyzed estimate of the core state,  $M\epsilon_i^a = M(\mathbf{x}_i^a - \mathbf{x}_i^t)$ . Even if estimated using previous observations, the estimate  $\mathbf{x}_i^a$  is not the true state of the core. The statistics of that component of the error field are described by the time-dependent, a priori error covariance matrix  $\mathbf{P}_i^a$ . We will assume again that the error has zero mean and that it is distributed as a Gaussian, multivariate random variable.
- The model error  $\eta_{i+1} = M\mathbf{x}_i^t - \mathbf{x}_{i+1}$ , which was already introduced in the previous paragraph, with covariance matrix  $\mathbf{Q}_{i+1}$ .

The statistical properties of the forecast error are described by a covariance matrix given by

$$\mathbf{P}_{i+1}^f = E(\epsilon_{i+1}^f \epsilon_{i+1}^{fT}) = M\mathbf{P}_i^a M^T + \mathbf{Q}_{i+1}, \tag{7}$$

<sup>5</sup> $\mathbf{x}_i^a$  is either the product of a previous assimilation cycle, or based on the initial guess trajectory in the case of the first encounter with an observation.

**Fig. 2** The forecast error  $\epsilon_{i+1}^f$  has two sources: One is related to the propagation of the a priori error by the model (*dashed arrow*), and the other is related to the model itself:  $\eta_{i+1}$  quantifies the physics which the model does not account for properly. After Brasseur (2006)



- in which  $E(\cdot)$  denotes statistical expectation and  $T$  means transpose. The error on the initial state is transformed during the forecast state by the model dynamics, and augmented by the model imperfections, both being assumed statistically independent.
- The analysis: The goal of the analysis is to determine the optimal estimate  $\mathbf{x}_{i+1}^a$  of  $\mathbf{x}_{i+1}^t$ , given the observations  $\mathbf{y}_{i+1}^o$ . The corresponding conditional probability  $p$  is given by Bayes' formula

$$p(\mathbf{x}_{i+1}^t | \mathbf{y}_{i+1}^o) = \frac{p(\mathbf{y}_{i+1}^o | \mathbf{x}_{i+1}^t) p(\mathbf{x}_{i+1}^t)}{p(\mathbf{y}_{i+1}^o)} \tag{8}$$

The numerator being a simple scaling factor, it can be ignored when trying to maximize that probability density function (pdf). Our hypotheses of Gaussianity imply

$$p(\mathbf{x}_{i+1}^t | \mathbf{y}_{i+1}^o) \propto \exp \left[ -\frac{1}{2} \left( \boldsymbol{\epsilon}_{i+1}^{oT} \mathbf{R}_{i+1}^{-1} \boldsymbol{\epsilon}_{i+1}^o + \boldsymbol{\epsilon}_{i+1}^{fT} \mathbf{P}_{i+1}^{f-1} \boldsymbol{\epsilon}_{i+1}^f \right) \right], \tag{9}$$

and finding the optimal estimation (which maximizes this expression) is equivalent to finding the minimum of the argument of the exponential. Given the expressions of the various error fields, the corresponding functional  $J$  writes

$$J(\mathbf{x}) = (\mathbf{y}_{i+1}^o - H_{i+1}\mathbf{x})^T \mathbf{R}_{i+1}^{-1} (\mathbf{y}_{i+1}^o - H_{i+1}\mathbf{x}) + (\mathbf{x}_{i+1}^f - \mathbf{x})^T \mathbf{P}_{i+1}^{f-1} (\mathbf{x}_{i+1}^f - \mathbf{x}). \tag{10}$$

After some algebra, one finds that the optimal estimation for the state vector,  $\mathbf{x}_{i+1}^a$ , is given by

$$\mathbf{x}_{i+1}^a = \mathbf{x}_{i+1}^f + K_{i+1} (\mathbf{y}_{i+1}^o - H_{i+1}\mathbf{x}_{i+1}^f), \tag{11}$$

in which

$$K_{i+1} = \mathbf{P}_{i+1}^f H_{i+1}^T (H_{i+1} \mathbf{P}_{i+1}^f H_{i+1}^T + \mathbf{R}_{i+1})^{-1} \tag{12}$$

is the so-called Kalman gain matrix. Two limits are of pedagogical interest: First, in the case of perfect observations ( $\mathbf{R}_{i+1} \sim \mathbf{0}$ ) of the entire state ( $H_{i+1} \sim \mathbf{I}$ ), the Kalman gain is the identity  $\mathbf{I}$ . Second, in the case of an extremely accurate forecast ( $\mathbf{P}^f \sim \mathbf{0}$ ), the correction to the forecast becomes negligible.

The analysis is in turn characterized by an error described by the covariance matrix

$$\mathbf{P}_{i+1}^a = [\mathbf{I} - K_{i+1} H_{i+1}] \mathbf{P}_{i+1}^f. \tag{13}$$

That last equation shows how the uncertainty in the forecast decreases in proportion to the amount of information added to the system.

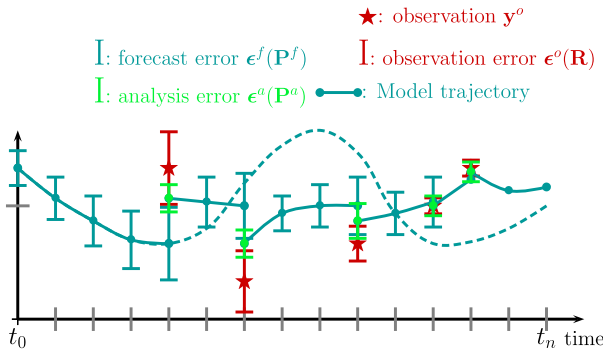


**Fig. 3** The sequential approach to data assimilation. Starting from the initial time, the model trajectory follows the initial forecast, and is characterized by a growth of the forecast error. As soon as the first observation is available, the analysis is performed (green bullet), and the associated error decreases (green error bar). The same cycle is repeated anytime an observation is available, with the assimilated trajectory deviating from the initial guess (the dashed line)

The innovation  $\mathbf{d}$  then represents the difference between the observations and the forecast

$$\mathbf{d}_{i+1} = \mathbf{y}_{i+1}^o - H_{i+1}\mathbf{x}_{i+1}^f, \tag{14}$$

while the residual  $\mathbf{r}$  refers to the difference between the same observations and the analysis

$$\mathbf{r}_{i+1} = \mathbf{y}_{i+1}^o - H_{i+1}\mathbf{x}_{i+1}^a. \tag{15}$$

These two fields are useful for assessing the a posteriori consistency of a data assimilation scheme (see Sect. 2.2.4).

To summarize, sequential assimilation consists first of a forecast stage, where both the forecast and (in principle) its error statistics are computed thanks to the model (see (5) and (7)). During the second stage, the available observations are used to correct the forecast and its error statistics, according to (11) and (13), respectively. That process is repeated sequentially, as illustrated schematically in Fig. 3.

Finally, recall that to get (7), we assumed that the model  $M$  was linear. If the assumed dynamics is non-linear, one has to replace  $M$  in that equation by the tangent linear model  $\mathbf{M}$ , obtained by linearizing the model about the current model trajectory. Equations (5), (11), and (13) still hold in the so-called extended Kalman filter (EKF) framework.

### 2.2.2 Variational Assimilation

Unlike sequential assimilation (which emanates from estimation theory), variational assimilation is rooted in optimal control theory. The analyzed state is not defined as the one maximizing a certain pdf, but as the one minimizing a functional  $J$  of the form

$$J(\mathbf{x}) = \frac{1}{2} \left\{ \sum_{i=0}^n [H_i\mathbf{x}_i - \mathbf{y}_i^o]^T \mathbf{R}_i^{-1} [H_i\mathbf{x}_i - \mathbf{y}_i^o] + [\mathbf{x} - \mathbf{x}^b]^T \mathbf{P}^{b-1} [\mathbf{x} - \mathbf{x}^b] \right\}, \tag{16}$$

in which  $\mathbf{x}_i = M_{i,i-1} \cdots M_{1,0}\mathbf{x}$ , the sought  $\mathbf{x}$  being the best estimate of the initial state of the core  $\mathbf{x}_0$ . This objective function is defined over the entire time window of interest. It is the sum of two terms. The first one measures the distance between the observations and the

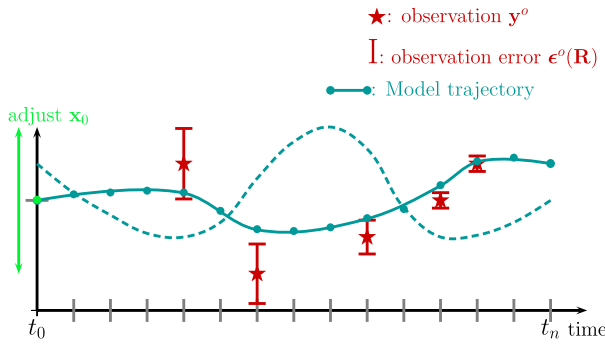


**Fig. 4** The variational approach to data assimilation. After adjustment of the initial condition  $\mathbf{x}_0$  (the green bullet on the  $t = t_0$  axis) by means of an iterative minimization algorithm, the model trajectory is corrected over the entire time window, in order to provide an optimal fit to the data (in a generalized least squares sense). The dashed line corresponds to the initial (unconstrained) guess of the model trajectory introduced in Fig. 1

predictions of the model. It is weighted by the confidence we have in the observations. The second term is analogous to the various norms which are added when solving the kinematic core flow problem; it evaluates the distance between the initial condition and an a priori background state  $\mathbf{x}^b$ . That stabilizing term is weighted by the confidence we have in the definition of the background state, described by the background error covariance matrix  $\mathbf{P}^b$ .<sup>6</sup> Defining a background state for the core is no trivial matter. But one may substitute (or supplement) the corresponding term in (16) by (with) another stabilizing term, typically a norm, as was done by Talagrand and Courtier (1987) and Courtier and Talagrand (1987) in their early numerical experiments with the vorticity equation on the sphere.

The goal of variational data assimilation is to minimize  $J$  by adjusting its control variables (or parameters), usually the initial condition  $\mathbf{x}_0$  (if everything else is held fixed, see Fig. 4), as implied by our formulation in (16). Iterative minimization requires the computation of the sensitivity (gradient) of  $J$  with respect to its control vector, which writes  $(\nabla_{\mathbf{x}_0} J)^T$  (the transpose is needed since  $\nabla_{\mathbf{x}_0} J$  is by definition a row vector). The value of  $L_x$  precludes a brute force calculation of the gradient (which would imply  $L_x$  realizations of the forward model over  $[t_0, t_n]$ ). Fortunately, as pointed out early on by Le Dimet and Talagrand (1986) and Talagrand and Courtier (1987), a much more affordable method exists: The so-called adjoint method, which is based on the integration of the so-called adjoint equation backward in time

$$\mathbf{a}_{i-1} = \mathbf{M}_{i-1,i}^T \mathbf{a}_i + H_{i-1}^T \mathbf{R}_{i-1}^{-1} (H_{i-1} \mathbf{x}_{i-1} - \mathbf{y}_{i-1}^o) + \delta_{i1} \mathbf{P}^{b-1} (\mathbf{x}_{i-1} - \mathbf{x}^b), \quad n \geq i \geq 1, \quad (17)$$

starting from  $\mathbf{a}_{n+1} = \mathbf{0}$ , where  $\mathbf{a}$  is the adjoint field, and  $\delta$  is the Kronecker symbol. The initial value of the adjoint field provides the sensitivity we seek:  $(\nabla_{\mathbf{x}_0} J)^T = \mathbf{a}_0$  (e.g. Fournier et al. 2007). Note that when writing (17), we assumed for simplicity that observations were available at every model time-step.

Equation (17) indicates that over the course of the backward integration, the adjoint field is fed with innovation vectors. Those vectors have an observational component

<sup>6</sup>Ide et al. (1997), and many others, use  $\mathbf{B}$  to denote that matrix, a notation which is preempted in our case by the magnetic induction.

( $H_{i-1}\mathbf{x}_{i-1} - \mathbf{y}_{i-1}^o$ ), and a departure-to-background component ( $\mathbf{x}_0 - \mathbf{x}^b$ ), these two contributions being weighted by the statistics introduced above. The adjoint model  $\mathbf{M}^T$  in (17) is the adjoint of the tangent linear model  $\mathbf{M}$  introduced previously in the context of the extended Kalman filter. The adjoint model has a computational cost similar to that of the forward model, and makes it possible to use an iterative minimization algorithm suitable for large-scale problems.

A few comments on the adjoint method are in order:

- It demands the implementation of the adjoint model  $\mathbf{M}^T$ : the rules to follow for deriving (and validating) the tangent linear and adjoint codes from an existing forward code are well documented in the literature (e.g. Talagrand 1991; Giering and Kaminski 1998), and leave no room for improvisation. Still, this process is rather convoluted. It requires expertise and deep knowledge of the forward code to begin with. The best situation occurs when the forward code is written in a modular fashion, bearing in mind that its adjoint will be needed in the future, and by casting as many operations as possible in terms of matrix-matrix or matrix-vector products (for a one-dimensional illustration with a spectral-element, non-linear magnetohydrodynamic model, see Fournier et al. 2007). The task of coding an adjoint by hand can still become beyond human reach in the case of a very large model. One might then be tempted to resort to an automated differentiation algorithm. Automated differentiation (AD) is a very active field of research:<sup>7</sup> several operational tools are now available, some of which have been tested on geophysical problems by Sambridge et al. (2007).
- The discrete adjoint equation (17) is based on the already discretized model of core dynamics. An alternative exists, which consists first in deriving the adjoint equation at the continuous level, and second in discretizing it, using the same machinery as the one used to discretize the forward model. In most instances, both approaches to the adjoint problem yield the same discrete operators. When in doubt, though, in the case of a minimization problem, one should take the safe road and derive the adjoint of the already discretized problem: This guarantees that the gradient injected in the minimization algorithm is exactly the one corresponding to the discrete cost function (16), up to numerical roundoff error. Since the efficiency of a minimization algorithm grows in proportion to its sensitivity to errors in the gradient, any error in the gradient could otherwise result in a suboptimal solution.
- The adjoint approach is versatile. Aside from the initial state  $\mathbf{x}_0$ , one can declare static model parameters (static fields, material properties) adjustable, and consequently part of the control vector. For example, Sect. 4.2 presents the results of twin (synthetic) experiments conducted with a torsional oscillation model, for which the control vector comprises the initial angular velocity and the static profile of the cylindrical radial component of the magnetic induction averaged over geostrophic cylinders.
- In the case of a non-linear problem, the forward trajectory  $\mathbf{x}_i$ ,  $i \in \{0, \dots, n\}$ , is needed to integrate the adjoint equation. The storage of the complete trajectory may cause memory issues (even on parallel computers), which are traditionally resolved using a so-called checkpointing strategy. The state of the system is stored at a limited number of discrete times, termed checkpoints. Over the course of the backward integration of the adjoint model, these checkpoints are then used to recompute local portions of the forward trajectory on-the-fly, whenever those portions are needed (e.g. Hersbach 1998).

<sup>7</sup>[www.autodiff.org](http://www.autodiff.org).

- On a more general note, adjoint methods have gained some popularity in solid Earth geophysics over the past few years, a joint consequence (again) of the increase in computational power and the availability of high-quality satellite, or ground-based, data. Adjoint methods are now applied to problems related to the structure and evolution of the deep Earth: Electromagnetic induction (Kelbert et al. 2008; Kushinov et al. 2010), mantle convection (Bunge et al. 2003; Liu and Gurnis 2008; Liu et al. 2008), and seismic wave propagation (Tromp et al. 2005, 2008; Fichtner et al. 2006), building in that last case on the theoretical work of Tarantola (1984, 1988).

The application of a variational approach to time-dependent problems has been generically labeled as the 4D-Var approach to data assimilation (e.g. Courtier 1997), and is commonly referred to as 4D-Var. As such, the standard 4D-Var suffers from two drawbacks: It assumes that the model is perfect ( $\eta = \mathbf{0}$ ), and it does not provide direct access to the statistics of the analysis error—notice its absence in Fig. 4. An alternative approach to the “strong constraint” assumption ( $\eta = \mathbf{0}$ ) consists in adding a term quantifying the model error in the definition of the cost function, a term whose weight is controlled by an a priori forecast error covariance. This more general “weak constraint” approach (Sasaki 1970) has been successfully introduced and implemented (under the name “method of representers”) in physical oceanography during the past fifteen years (Egbert et al. 1994; Bennett 2002, and references therein). It allows in particular the derivation of posterior error covariances (see also Uboldi and Kamachi 2000). An interesting discussion on various approaches to “weak constraint” 4D-Var in an operational context is also provided by Trémolet (2006).

From a general perspective, the advantages of a variational approach are its flexibility regarding the definition and identification of control variables, and its natural ability to handle time-dependent observation operators (and possibly time-correlated errors). It is also well-suited for the reanalysis of past data records (hindcasting), since the state at a given time is estimated using the past and future observations available over the entire time window (see Fig. 4). Note, however, that hindcasting is also possible if one resorts to sequential smoothers, of the kind described by e.g. Cohn et al. (1994), and applied in an oceanic context by e.g. Cosme et al. (2010).

### 2.2.3 Practical Considerations: Non-linearities, Size, Cost

Sequential and variational assimilations share the same goal. As suggested by the definitions of the cost functions in (10) and (16), they are equivalent in the linear Gaussian case (Lorenz 1986). In a weakly non-linear situation (and still assuming Gaussian statistics), the equivalence holds at first order between the EKF and 4D-Var, since both resort to the same tangent linear model  $\mathbf{M}$  (Courtier 1997). In a strongly non-linear case, issues arise in both approaches.

From the variational point of view, the cost function can lose its convexity, and several local minima exist. This situation is illustrated in a 1-parameter synthetic situation in Fig. 5. In that example, a reference secular variation is generated using the frozen-flux equation (1). It is initialized by a given map of  $B_r$  at the top of the core, and is due to an equatorially symmetric quasi-geostrophic  $u_h$ . The secular variation is generated over a time window of variable width  $T$ , expressed in units of the advective time  $T_{\text{adv}}$ , defined as the ratio of the outer core radius  $c$  to the rms flow speed  $U$  (see Table 3). The control vector is reduced to a single scalar, which prescribes the position of a mid-latitude cyclonic vortex (located along the Greenwich meridian in the reference, i.e. ‘true’, case, see Fig. 5). We generate a collection of guesses of the secular variation by picking the same initial  $B_r$  and letting the

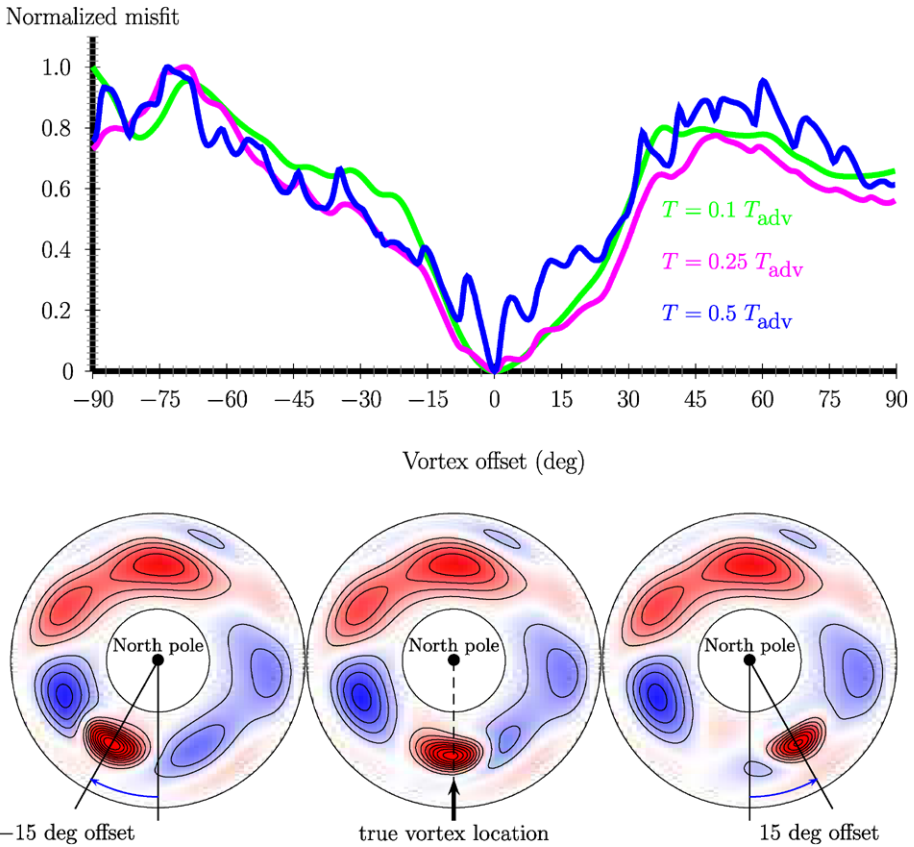


**Fig. 5** In the synthetic context of a secular variation generated by a steady quasi-geostrophic core flow  $u_h$ , the three curves on the top represent the misfit between a reference frozen-flux secular variation, due to a true flow  $u_h^t$ , and a frozen-flux secular variation due to a guess flow  $u_h^g$  (both secular variations are initialized with the same  $B_r$  at the top of the core); the only difference between  $u_h^t$  and  $u_h^g$  is the longitude of the eye of a mid-latitude Gaussian vortex of half-width  $c/10$ , where  $c$  is the radius of the outer core. The streamfunction associated with  $u_h^t$  is represented in the *middle of the bottom row* (in the equatorial plane, looking from the North pole). It is based on a solution obtained by Gillet et al. (2009), with a peak-to-peak amplitude on the order of roughly  $15,000 \text{ y}^{-1}$ , which yields an rms velocity of order  $15 \text{ km/y}$ . Red and blue correspond to cyclonic and anti-cyclonic motions, respectively. The streamfunctions shown to the *left and right* of the true streamfunction are guesses for which the vortex offset is  $-15$  degrees and  $+15$  degrees, respectively ( $+$  means Eastward). In the *top*, the misfit is plotted as a function of the offset longitude in degrees, for three different time window widths  $T$ :  $0.1$ ,  $0.25$ , and  $0.5$  advective time  $T_{adv}$  (the *green, magenta, and blue curves*, respectively). The three curves have been normalized to ease cross-comparison. The global minimum (when the guessed flow is the true flow, i.e. the offset is zero) is set in a valley which gets narrower as  $T$  is increased, indicating that in an inversion setting, an inaccurate initial guess for the vortex location could result in a solution corresponding to an undesired local minimum

position of this vortex vary (as illustrated on the maps in the bottom of Fig. 5), and estimate the misfit between the reference secular variation and every single guess. Fig. 5 (top) shows the misfit as a function of the vortex offset for three different time window widths  $T$ :  $0.1$ ,  $0.25$ , and  $0.5$  advective time  $T_{adv}$  (the *green, magenta, and blue curves*, respectively). The three curves have been normalized to ease cross-comparison. The global minimum (when the guessed flow is the true flow, i.e. the offset is zero) is set in a valley which gets narrower

as  $T$  is increased. In addition, the number of local minima (the wiggly character of the misfit) increases substantially with  $T$ . This example indicates that in the context of a gradient-based search, an inaccurate initial guess can result in a solution corresponding to a local minimum if the inversion is carried out over a time window of width  $T$  representing a substantial portion of the time scale of the dynamics at work (the advective time in our example).

From the sequential point of view, propagating the error statistics via (7) using  $\mathbf{M}$  can lead to poor error covariance evolution and even unstable error covariance growth (Miller et al. 1994). This growth is intrinsically related to the chaotic underlying dynamics. In that case, no assimilation should be undertaken over time windows of width larger than the intrinsic predictability time limit for the system, whose value is governed by the combined effects of, first, the amplitude of the error with which the state is estimated from the observations, and, second, the intrinsic error growth rate  $\lambda_e = \tau_e^{-1}$  resulting from the chaotic dynamics (Sect. 4.3 discusses further the value of the  $e$ -folding time  $\tau_e$  for the geodynamo).

A remedy to an unstable covariance error growth exists, which relies on a probabilistic description of the non-linear evolution of the model state, and the associated time-dependent pdf based upon a well-chosen ensemble of non-linear forward realizations (Evensen 1994): The so-called ensemble Kalman filter (EnKF) is described in great detail by Evensen (2009), and a first example of a simple application in geomagnetism is that of Beggan and Whaler (2009). Since the time-dependent forecast error covariance matrix is directly derived from the ensemble of forecasts, the EnKF has the extra advantage of making (7) and (13) obsolete: The awfully expensive propagation of error statistics<sup>8</sup> is no longer needed. Actually, the horrendous cost of error statistics propagation often leads data assimilation practitioners to employ a static (frozen) background error covariance matrix, by setting  $\mathbf{P}_i^f = \mathbf{P}^b$  for all discrete times: That popular approach is referred to as optimal interpolation (OI), although the convenient approximation upon which it rests makes it suboptimal (e.g. Brasseur 2006). It is, however, a good approximation to begin with, before embarking on more sophisticated strategies such as the EnKF. Section 4.1 presents results obtained in an OI framework by assimilating geomagnetic field models with a three-dimensional model of the geodynamo.

In terms of computer resources, assimilation is very demanding, especially when dealing with non-linear dynamics. For OI and EnKF, the derivation of good error statistics requires an ensemble size of order  $\mathcal{O}(10\text{--}100)$ . Conversely, for 4D-Var, the iterative non-linear minimization might also be achieved in several tens of iterations, bearing in mind that a given iteration relies on a forward and an adjoint calculation. Good preconditioning is therefore almost mandatory. For geomagnetic data analysis, a solution to circumvent the cost problem consists in simplified dynamical models, of reduced dimensionality, and tailored to the study of the secular variation, an example of which is provided in Sect. 4.2.

The computational cost is roughly the same for sequential and variational assimilations.<sup>9</sup> The former is easier to implement than the latter, at the expense of the loss of some flexibility. For an interesting and animated discussion on the relative merits of 4D-Var and the EnKF under their most recent and sophisticated implementations, the reader is referred to Kalnay et al. (2007a, 2007b) and Gustafsson (2007). As far as geomagnetic data assimilation is concerned, and because it is still in its infancy, let us bear in mind for the time being that key to the success of both approaches is a good, trustworthy description of error statistics.

<sup>8</sup>A quick inspection of equations (5) and (7) shows indeed that the propagation of error statistics is  $L_{\mathbf{x}}$  times more expensive than a model step, a factor which is prohibitive for almost any practical application, starting from  $L_{\mathbf{x}} \gtrsim 1,000$ , say.

<sup>9</sup>In an operational setting, and at the same computational cost, Buehner (2008) reports that weather forecasts based either on 4D-Var or the EnKF perform equally well.



2.2.4 *A Posteriori Validation, Statistical Consistency and Possible Model Bias*

Once a data assimilation scheme has been implemented, it is possible to perform a posteriori quality and consistency checks to evaluate its performance, and assess the robustness of the hypotheses upon which it relies. These checks are reviewed by Brasseur (2006) in the monograph edited by Chassignet and Verron (2006) and by Talagrand (2003), to which the reader should refer for further detail and references. One intuitive way to assess the efficacy of a given scheme is to compare its predictions with independent measurements of the state of the system. In the oceanographic context, these can consist of measurements of the state of the ocean obtained via a network of buoys. The Earth’s core does not lend itself easily to that type of practice, given the sparse database of observations at hand (see Sect. 3 below). Nevertheless, independent and reliable observatory timeseries and the interannual to decadal variation of the length of day (which is related to the angular momentum carried by the core flow, Jault et al. 1988; Jackson et al. 1993) appear as natural candidates for this exercise.

It is also possible to perform internal consistency checks. For instance, in a sequential framework, the first-order moment of the innovation vector (defined in (14)) should vanish over a sufficiently long assimilation sequence

$$E(\mathbf{d}_i) = E(\mathbf{y}_i^o - H_i \mathbf{x}_i^f) = E\left[H_i \mathbf{x}_i^t + \boldsymbol{\epsilon}_i^o - H_i(\mathbf{x}_i^t + \boldsymbol{\epsilon}_i^f)\right] = E(\boldsymbol{\epsilon}_i^o) - E(H_i \boldsymbol{\epsilon}_i^f) = \mathbf{0}, \tag{18}$$

in which we have used the definitions of the error fields introduced above, and assumed (as usual) that both were centered. Note that in practice the expectation is computed by taking the time average, i.e. the algebraic mean over all the discrete times  $t_i$  at which an assimilation cycle is performed (see the interesting discussion about this practical necessity in Dee and Da Silva 1998). The same property should hold in the variational case, provided the innovation is defined as the difference between the observations and the predictions based upon the estimate of background state  $\mathbf{x}^b$  (Talagrand 2003).

A non-zero mean innovation points at a bias, in the observation error or/and in the model error. In case the bias comes from the model,  $E(\mathbf{d}_i)$  provides only the projection of this bias onto the data space, which for the geomagnetic field is restricted to the largest scales of the field at the core-mantle boundary (see Sect. 3 below). Therefore, in the context of geomagnetism, it appears crucial to choose a model that possesses at least some degree of similarity with what we see of the true geomagnetic field. This is necessary if we do not want to deal with a forecast bias, by resorting to a dynamical forecast bias removal strategy such as the one favoured by Dee and Da Silva (1998).

If the model is a three-dimensional model of the geodynamo, we note that in a recent study, Christensen et al. (2010) define a series of quantitative static criteria to help define what would be a good candidate model to represent the geomagnetic field. They consider the ratio of the power in the axial dipole component to that in the rest of the field, the ratios between equatorially symmetric and antisymmetric and between zonal and non-zonal non-dipole components, and a measure for the degree of spatial concentration of magnetic flux at the core surface. Again, these criteria are purely morphological and static; other dynamical properties could be sought, such as the existence of a significant secular variation occurring in the equatorial region, and a tendency for a westward drift of magnetic structures (at least in the Atlantic hemisphere).

The first-order moment of the residual vector (defined in (15)) should also vanish. Should it not, it would hint at the sub-optimality of the system (Talagrand 2003). Many more criteria exist, which involve for instance the second-order moments of the innovation and residual vectors. Here we simply refer the reader to the references listed above for an extensive

coverage of these quality checks (see also Bennett 2002, Sect. 2.3.3). As far as we know, such criteria have not yet been applied to geomagnetic data assimilation schemes, but they should certainly come to the fore when the field becomes more mature, given the insight they can provide (in particular regarding the model bias).

### 3 Geomagnetic Observations and Their Connection with the State of the Core

Having introduced the basics of data assimilation, let us now try to provide the reader with an overview of the geomagnetic observations  $\mathbf{y}^o$  which are in principle amenable to geomagnetic data assimilation practice. We do not aim at discussing here the observation errors (the content of the matrix  $\mathbf{R}$ ), an account of which can be found in the reviews by Hulot et al. (2007), Jackson and Finlay (2007), and Hulot et al. (2010b) for the archeomagnetic database. Rather, we focus on the issue of relating those observations to the state of the core. The keypoint for us is that those measurements are in all cases related to the knowledge of the radial component of the magnetic induction at the top of the core,  $B_r$ . We will accordingly discuss the nature of the observation operator  $H$  associated with a given measurement.

Modern geomagnetic data consist of appropriately processed time series of the three components of  $\mathbf{B}$ , usually recorded in observatories or by dedicated satellites (see Fig. 6). Those “level-1B”-type data, in space agency parlance, are the observations one would ultimately like to assimilate. At a given location  $\mathbf{r}^o$ , however, the measured field results from the contribution of several internal and external sources (core, crust, ionosphere, magnetosphere, the world ocean), and further time and space filtering is therefore required to isolate the (dominant) signal originating from the core. Various techniques can be used, depending on the type, quantity and quality of data considered. In particular, whereas contributions from non-core sources can only be dealt with as a source of noise when considering early historical data (see e.g. Jackson and Finlay 2007), more advanced techniques have been designed for observatory time series and even more so for satellite data (see e.g. Hulot et al. 2007). In that case, the core field contribution of interest is often directly provided in the form of a so-called geomagnetic field model, which consists in a time-varying spherical harmonic description of the core field. Such models are usually referred to as “level-2” data (products) in space agency parlance.

Practically speaking, and assuming an electrically insulating mantle (a reasonable first-order approximation, see e.g. Alexandrescu et al. 1999), the connection between the state of the core  $\mathbf{x}$  (which comprises in some form  $B_r$  at the core surface  $S$ ) and an estimate  $B_\alpha$  ( $\alpha = 1, 2, 3$ ) of the core field at  $\mathbf{r}^o$  is achieved by means of a data kernel  $K_\alpha$

$$B_\alpha(\mathbf{r}^o) = \int_S K_\alpha(\mathbf{r}^o, \mathbf{r}) B_r(\mathbf{r}) d^2\mathbf{r}, \quad (19)$$

where  $\mathbf{r}$  denotes a point at the core surface  $S$  (see e.g. Gubbins and Roberts 1983; Bloxham et al. 1989; Jackson 1989, for explicit expressions of these kernels). The exact discrete form of the observation operator  $H$  (which is linear in this case) depends ultimately on the quadrature rule used to evaluate the above integral.

Some data (in particular early historical and observatory data) are however sometimes only available in the form of individual inclination and declination measurements. Those are non-linearly related to the components  $B_\alpha$ . Directly assimilating such data implies dealing with a non-linear observation operator  $H$ . The machinery presented in Sect. 2 remains nevertheless applicable, provided a linearization of  $H$  about the current state of the core (or

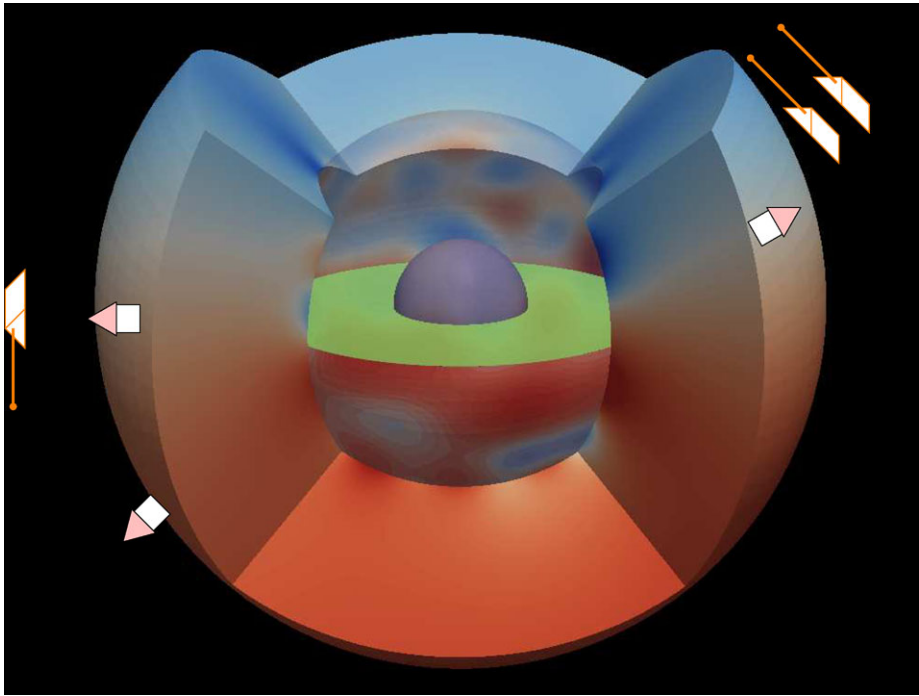


**Fig. 6** The magnetic observation of the Earth is made possible by an unevenly distributed network of long-lived magnetic observatories located at its surface. The corresponding database has been supplemented over the past few decades by satellite measurements, most notably during the past ten years for which a continuous satellite database is available. The global coverage provided by the satellites ideally complement the longer observatory time series. In this figure, the innermost sphere is the inner core, which is surrounded by the outer core. The *green plane* is the equatorial plane. The color scale at the core-mantle boundary represents the radial component of the magnetic induction  $B_r$  at epoch 2004, according to the CHAOS model of Olsen et al. (2006), with a typical amplitude of  $\pm 1$  mT. Going from the surface of the core to the surface of the Earth through the mantle (two thirds of which are represented here), the field decreases. The smaller scales decrease most rapidly, which yields an almost dipolar structure at the surface of the Earth, with the field lines pointing outward in the Southern hemisphere (positive, *red*  $B_r$ ) and inward in the Northern hemisphere (negative, *blue*  $B_r$ ). The field amplitude at a given location radius  $r$  has been scaled by a factor  $(r/c)^3$  for the sake of visibility,  $c$  being the radius of the outer core

the background guess, in a weakly non-linear case) is performed, and an iterative solution sought.

On another note, it is also in principle possible to account for the finite electrical conductivity of the mantle  $\sigma_m$ , which introduces a delay between an event occurring at the core surface and its signature at the surface of the Earth. Mantle filter theory (e.g. Backus 1983) requires to replace the kernels in (19) by more general impulse response functions  $F_\alpha$  (whose exact form depends on the distribution of  $\sigma_m$  in the mantle), and to convolve these with the history of the evolution of  $B_r$  on  $S$

$$B_\alpha(\mathbf{r}^o, t) = \int_0^t \int_S F_\alpha(\mathbf{r}^o, \mathbf{r}, t - \tau) B_r(\mathbf{r}, \tau) d^2\mathbf{r} d\tau. \tag{20}$$

Implementing such a formalism would be most useful for the investigation of short time scale core dynamics (sub-annual to interannual, say), for which delay and attenuation could

have some importance when trying to interpret the data (e.g. Pinheiro and Jackson 2008). But this calls for substantial novel methodological developments.

Another issue of more immediate concern is the concealing of the smallest spatial scales of the core field by the crustal field. It is related to the formal impossibility of distinguishing the contribution of magnetized sources located within the crust from that of the core. It is well-known that at any given time the core field dominates the largest spatial scales (roughly up to spherical harmonic degree 14, which corresponds to 800 km at the core surface  $S$ ), whereas the crustal field dominates the smallest spatial scales (e.g. Hulot et al. 2007). This concealing not only affects the field itself but also its time derivative (the secular variation), the smallest scales of which are again expected to be dominated by the crustal secular variation (Hulot et al. 2009). In that case, however, the transition is expected to occur further down the spectrum (near spherical harmonic degree 18, corresponding to a length scale of 600 km on  $S$ ); this leaves some room for improvement compared to the current situation where the core field secular variation is perhaps recovered up to degree 16 (e.g. Olsen and Mandaia 2008). Such an improvement can be expected from the upcoming ESA SWARM mission (Friis-Christensen et al. 2006).<sup>10</sup> The myopia of the geomagnetic observer interested in the core field is a disease which has long been diagnosed. It can be mitigated by resorting to averaging kernels (e.g. Whaler and Gubbins 1981; Jackson 1989; Backus et al. 1996, §4.4.4), and replacing effectively  $B_r$  in (19) by an appropriately averaged  $\hat{B}_r$  (see also Canet et al. 2009).

Geomagnetic data assimilation is still in its early days and, to our knowledge, a study assimilating “true” geomagnetic observations  $y^o$  remains to be seen. Instead, researchers have so far cautiously dealt with synthetic data (for algorithmic verification), and with published core geomagnetic field models. These models provide parameterized time-dependent maps of  $B_r$  at the core surface (through a set of time-dependent Gauss coefficients), and over different time scales, ranging from a decade to several centuries (e.g. Lesur et al. 2008; Olsen et al. 2006; Sabaka et al. 2004; Jackson et al. 2000). Models covering up to several millennia have also been built thanks to the availability of archeomagnetic data (see e.g. Hongre et al. 1998; Korte and Constable 2005; Korte et al. 2009). The accuracy of those models degrades going back in time, as a result of the temporal and spatial sparsity, and greater uncertainty, of the data they rely on. In addition, prior to 1850, historical models are mostly based on directional measurements (Jackson et al. 2000), which makes it possible to recover the field morphology (Hulot et al. 1997), but precludes the determination of the global strength of the field. Still, there is an encouraging ongoing effort to improve on that situation thanks to the construction of archeomagnetic intensity databases (e.g. Genevey et al. 2008). In particular, careful intensity measurements covering the period 1590–1850 could prove useful in complementing the data already extracted from logbooks (Gubbins et al. 2006; Finlay 2008; Genevey et al. 2009).

In Table 2, we have tried to synthesize the information content already available for geomagnetic data assimilation. We computed the average size  $L_{y^o}$  of the data vector that could be fed in an assimilation scheme over different time periods, assuming a model of core dynamics operating with a time-step of 1 week, and relying on the number of data used to construct the field models referenced in the rightmost column. As graphically shown in Fig. 7, the last decade of satellite measurements allows for a dramatic tenfold increase in the size of  $y^o$ . In a variational framework aiming at adjusting the initial condition (see Sect. 2.2.2), the size of the control vector (the initial state  $\mathbf{x}_0$ ) for a typical, three-dimensional dynamo

<sup>10</sup>[www.esa.int/esaLP/ESA3QZJE43D\\_LPswarm\\_0.html](http://www.esa.int/esaLP/ESA3QZJE43D_LPswarm_0.html).

**Table 2** An attempt to summarize the observational content available to geomagnetic data assimilation practitioners. We took the number of data (and corresponding timespan) used in the studies listed in the rightmost column to estimate the average quantity  $L_{y^o}$  of observations that could be fed in an assimilation scheme at every single time-step, assuming a numerical model of core dynamics operating with a time-step  $\Delta t = 1$  week

Period	Average $L_{y^o}$	Type of data	Reference
2000–now	10,000	observatory & satellite	Lesur et al. (2008)
1960–2002	1,000	observatory & satellite	Sabaka et al. (2004)
1900–1960	50	observatory & satellite & survey	Jackson et al. (2000)
1600–1900	10	navigation & observatory	Jackson et al. (2000)
0–1600	0.1	archeomagnetic	Korte and Constable (2005)

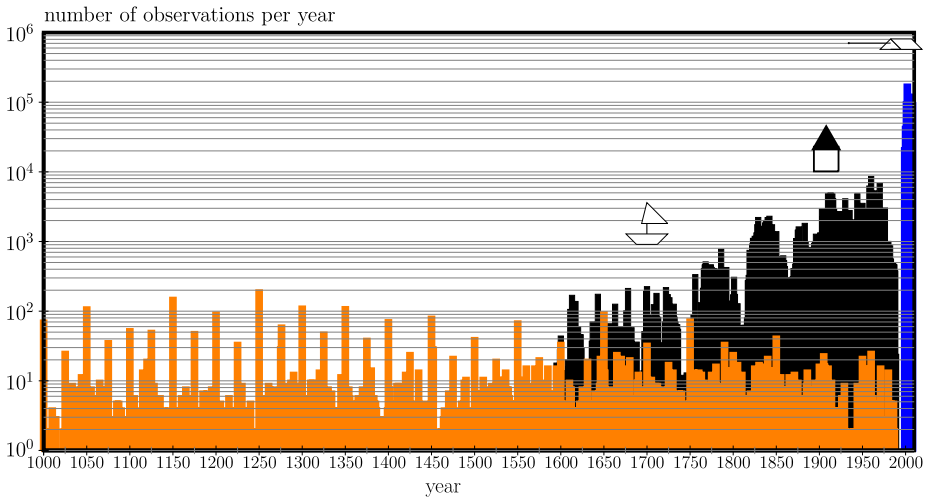


**Fig. 7** Amount of geomagnetic measurements available over the last millennium, from archeomagnetic sources (orange bars), historical sources (black bars), and from the recent satellite era (blue bars). The data have been binned in bins of 1 year, and the scale on the y axis is logarithmic. The archeomagnetic curve has been constructed using the Geomagia database, available online at [geomagia.ucsd.edu](http://geomagia.ucsd.edu) (Korhonen et al. 2008; Donadini et al. 2009). The historical curve is that of the gufm model of Jackson et al. (2000), and the recent satellite curve is based on the xCHAOS model of Olsen and Mandea (2008)

model is of order 1 million.<sup>11</sup> Table 2 encouragingly indicates that two years of satellite data suffice to get a number of observations similar to the size of the control vector. A note of caution is in order, though: At any given time  $t_i$ , the number of observations will certainly not exceed the size of the state vector. It is the accumulation of observations over time which is such that their total number will eventually exceed the size of the state vector (and make the minimization problem of variational assimilation “appear” well determined). As seen above, the effective part of the control vector directly sampled by observation involves at

<sup>11</sup>Follow the pseudo-spectral approach of Glatzmaier (1984) and perform the poloidal-toroidal decomposition of flow and magnetic field. The state vector  $\mathbf{x}$  then comprises the four corresponding scalar fields, augmented with temperature (or co-density). Operating with 80 Chebyshev polynomials in radius and a spherical harmonic expansion truncated at degree and order 50 to discretize the components of  $\mathbf{x}$  yields  $L_{\mathbf{x}} \approx 10^6$ .

most the first 15 spherical harmonic degrees of the poloidal field at the core-mantle boundary. From the spectral point of view (assuming a horizontal truncation at spherical harmonic degree 50, and 80 points in radius), that amounts to a modest 0.2 per mil of the state vector. However, that static estimate effectively increases by virtue of the dynamics (although that effect is hard to quantify), in the first place through the diffusive and convective transport of information which results from running the forward (or adjoint) model. The correction applied at the top of the dynamo region is communicated to the bulk of the core (through the action of either the Kalman gain or the adjoint model in a 4D-Var framework). This propagation can be made even more effective if multivariate statistics (relating observed and non-observed components of the state vector) are used to construct the background error covariance matrix  $\mathbf{P}^b$  (which appears in both the sequential and variational formulations of data assimilation).

Not surprisingly, it is over the historical period, and in particular the twentieth and early twenty-first centuries, that the first data assimilation studies have been attempted. The high quality and quantity of magnetic measurements available over that period imply in turn some confidence in the field models, which can be used as reasonable proxy “observations”. From the underlying core dynamics point of view, a century is also long enough to try and understand the fast variability of the geomagnetic secular variation. Dealing with time series of the Gauss coefficients also has a practical advantage: If the model of core dynamics  $M$  is discretized by means of spherical harmonics in the horizontal direction, then  $H$  very conveniently reduces to a diagonal operator (see e.g. Kuang et al. 2009).

We conclude this section by adding that an extra (geodetic) observation can be included in a geomagnetic data assimilation scheme. The time series of the fluctuation in the length-of-day ( $\Delta\text{LOD}$ ) has an annual to decadal component which is usually attributed to fluctuations in the core angular momentum (Jault et al. 1988; Jackson et al. 1993; Pais and Hulot 2000; Gillet et al. 2009). The construction of the component of  $H$  which is associated with the  $\Delta\text{LOD}$  signal is straightforward (it is linear).

#### 4 Current Approaches to Geomagnetic Data Assimilation

Different approaches to geomagnetic data assimilation have recently come to the fore in geomagnetism. Early studies have focussed on the feasibility of implementing data assimilation algorithms to the problem of the geomagnetic secular variation, by analyzing the response and behaviour of the assimilating system in a well-controlled environment, using databases of synthetic observations, starting from one-dimensional toy models (Fournier et al. 2007; Sun et al. 2007), and moving on to systems of higher complexity (Liu et al. 2007; Kuang et al. 2008; Canet et al. 2009). Those studies are generically referred to in the literature as “observing system simulations experiments” (OSSEs), or, equivalently, “twin experiments”. More recent applications have considered “level-2” observations (see Sect. 3 above), thereby permitting to make some inference on the state of the core  $\mathbf{x}$  (Kuang et al. 2009). The approaches followed nowadays differ by the choice of the physical and numerical model  $M$  employed to describe core dynamics, and the form of assimilation they resort to (sequential or variational). In this section, we shall give an example of a sequential approach based on a three-dimensional geodynamo model, followed by an example of a variational scheme designed for a two-dimensional quasi-geostrophic model of the secular variation; we will conclude with a discussion of the intrinsic limit of the predictability of the secular variation, as inferred from the results of a suite of three-dimensional dynamo models.

**Table 3** Summary of the various core dynamics-related symbols appearing in the text, and the non-dimensional numbers coming into play. Expressions that follow for the Ekman, Roberts, Rossby, and Rayleigh numbers, are obtained using the outer core radius  $c$  as the length scale, the magnetic diffusion time  $= c^2/\lambda$  as the time scale,  $(2\rho\lambda\mu\Omega)^{1/2}$  as the magnetic field scale, and  $h_T c$  as the temperature scale

Symbol	Meaning
$\rho$	core density
$\sigma_e$	electrical conductivity
$\mu$	magnetic permeability
$\lambda$	magnetic diffusivity $= 1/\mu\sigma_e$
$\nu$	kinematic viscosity
$\kappa$	thermal diffusivity
$\alpha_T$	thermal expansion coefficient
$\Omega$	the angular velocity of the Earth
$c$	outer core radius
$b$	inner core radius
$d$	outer core depth $= c - b$
$\mathbf{B}$	the magnetic induction (field)
$\mathbf{u}$	the core flow
$\Theta_0$	background temperature profile
$\Theta$	temperature anomaly
$h_T$	prescribed background temperature gradient $= -\partial_r \Theta_0 (r = b)$
$g_0$	the gravity field at $r = b$
$\mathbf{u}_h$	core surface flow
$\Psi$	geostrophic streamfunction
$B_0$	magnetic field scale
$U$	velocity scale
$\tau$	time scale
$T_{adv}$	advective time scale $\doteq c/U$
$V_A$	Alfvén wave speed $\doteq B_0/\sqrt{\rho\mu}$
$T_A$	Alfvén wave period $= c/V_A$
$E$	Ekman number $\doteq \nu/2\Omega c^2$
$q_\kappa$	Roberts number $\doteq \kappa/\lambda$
$Ro$	Rossby number $\doteq \lambda/2\Omega c^2$
$R_{th}$	Rayleigh number $\doteq \alpha_T g_0 h_T c^2/2\Omega\lambda$
$Rm$	magnetic Reynolds number $\doteq U c/\lambda$
$Pm$	magnetic Prandtl number $\doteq \nu/\lambda$
$Pr$	Prandtl number $\doteq \nu/\kappa$
$Le$	Lehnert number $\doteq B_0/c\Omega\sqrt{\rho\mu}$

A summary of the relevant quantities and notations we shall need is provided in Table 3. The Earth’s outer core is considered as a conducting fluid of density  $\rho$ , electrical conductivity  $\sigma_e$ , magnetic permeability  $\mu$ , magnetic diffusivity  $\lambda = 1/\mu\sigma_e$ , thermal diffusivity  $\kappa$ , and kinematic viscosity  $\nu$ . Owing to thermal-compositional convection (treated under the Boussinesq approximation) in an ambient gravitational field  $\mathbf{g}$ , the fluid flows at velocity  $\mathbf{u}$  and sustains a magnetic field (induction)  $\mathbf{B}$ . It is contained in a (to first order) spherical shell of inner radius  $b$  and outer radius  $c$ , corresponding to the inner-core boundary and core-mantle boundary, respectively. The core rotates about the  $z$ -axis (unit vector  $\mathbf{e}_z$ ) with an angular velocity  $\Omega$ . After proper non-dimensionalization, the numerical description of its dynamics is provided by a numerical model  $M$  which expects, aside from an initial con-



dition, a set of non-dimensional input parameters, the exact nature of which depends on the scales chosen for length, time, flow, and magnetic field (see Table 3).

#### 4.1 Sequential Assimilation Using Three-dimensional Models of the Geodynamo

Non-linear self consistent numerical dynamo models which are capable of generating an Earth like geomagnetic field have been in existence for a little more than a decade (Glatzmaier and Roberts 1995; Kageyama and Sato 1997; Kuang and Bloxham 1997). While computational limitations do not allow these models to operate in parameter regimes near those of the Earth's core, they are able to produce important physical processes such as dipole dominant poloidal magnetic field, westward drift and occasional field reversals (Christensen and Wicht 2007). However, if we look into the more detailed structures of the geomagnetic field from the dynamo solutions and from the observations, we will find they are very different, as shown in Fig. 8. Obviously, the model outputs are still very far away from those observed at the Earth's surface.

In many ways, these dynamo models are far more successful than the early numerical weather prediction models discussed in Sect. 1.2. But, again, a much bigger difference is

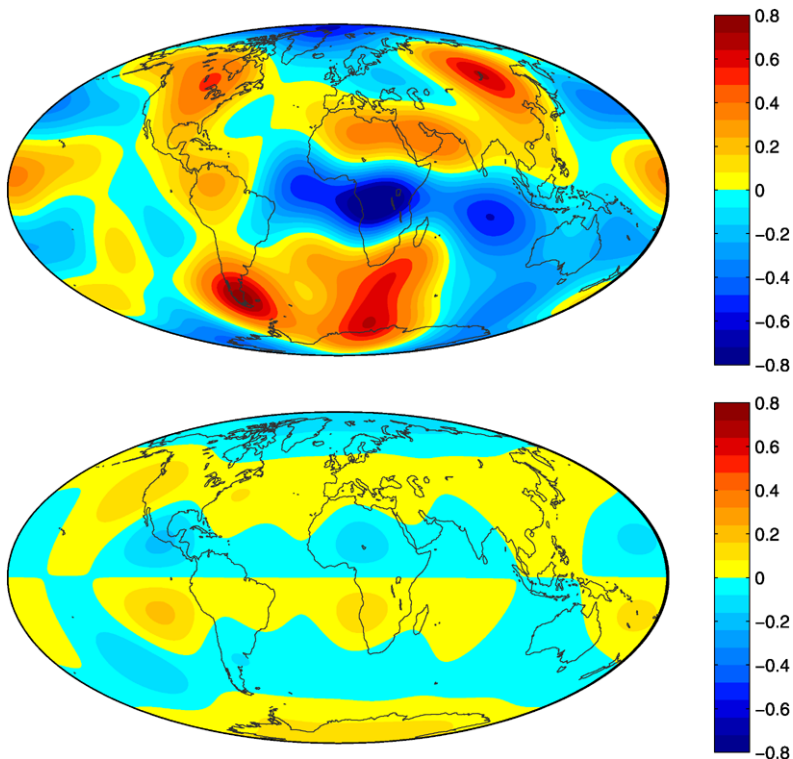


**Fig. 8** The non axial dipolar part of the radial component  $B_r$  of the magnetic field at the CMB from observation in 2000 according to the CM4 model of Sabaka et al. (2004) (*top*) and from the numerical dynamo simulation (*bottom*). The poloidal scalar (of the magnetic field) is expanded in spherical harmonics, with complex coefficients  $b_l^m$  of degree  $l$  and order  $m$ . Plotted in this figure are the scaled poloidal fields based on the spectral coefficients  $\bar{b}_l^m \equiv b_l^m/b_1^0$ , for all  $m \leq l \leq 8$ , and without  $(l, m) = (1, 0)$ . From Kuang et al. (2009)



that in geomagnetic data assimilation, the observations are only made at the surface of the Earth, and even then, only of the poloidal magnetic field. The observation vector  $\mathbf{y}^o$  therefore has a far smaller dimension than the state vector  $\mathbf{x}$ . If we carry out the assimilation in spectral space, and the maximum wave number that can be reliably assimilated is around  $l = 13$ , the observation operator  $H$  essentially acts to project the state space onto the smaller set of observations. State space (or model space) is defined as the magnetic field ( $\mathbf{B}$ ), velocity field ( $\mathbf{u}$ ) and the temperature perturbation ( $\Theta$ ) within the liquid outer core, with the velocity and magnetic fields further decomposed into poloidal and toroidal components. The only observations of the state are of the poloidal component of the magnetic field at the Earth's surface. The observations can then be downward continued to the dynamo domain boundary (DDB), e.g. the core-mantle boundary (CMB) or the top of the electrically conducting  $D''$ -layer (above the CMB). Therefore the observation operator is simply a matrix which projects the complete state space to the poloidal component of the magnetic field at the DDB.

The model  $M$  from (2) is in this case the discretization of the momentum, induction and energy equations, which in non-dimensional form are (see Table 3):

$$\text{Ro}(\partial_t \mathbf{u} + \mathbf{u} \cdot \nabla \mathbf{u}) = -\mathbf{e}_z \times \mathbf{u} - \nabla p + \mathbf{j} \times \mathbf{B} + \text{R}_{\text{th}} \Theta \mathbf{r} + \text{E} \nabla^2 \mathbf{u}, \tag{21}$$

$$\partial_t \mathbf{B} = \nabla \times (\mathbf{u} \times \mathbf{B}) + \nabla^2 \mathbf{B}, \tag{22}$$

$$\partial_t \Theta = -(\mathbf{u} \cdot \nabla) \Theta_0 - (\mathbf{u} \cdot \nabla) \Theta + \text{q}_\kappa \nabla^2 \Theta. \tag{23}$$

These equations have been solved by both finite difference (Kageyama and Sato 1997), combined spherical harmonics and Chebyshev polynomials (Glatzmaier and Roberts 1995) and combined spherical harmonics and finite differences (Kuang and Bloxham 1997).

A sequential data assimilation system has been built using the Kuang and Bloxham model (Kuang et al. 2008). This system features two possible means to estimate the forecast error covariance,  $\mathbf{P}^f$ , which are ensemble methods (Sun et al. 2007) and modeling. Ensemble estimation of forecast error covariance has enabled the construction of multivariate error covariances which allow the assimilation of the poloidal magnetic field to directly impact other state variables. Modeled covariances are constructed by choosing functions that result in error covariances that have the required properties of diagonal dominance and positive semi-definiteness (e.g. Gaspari and Cohn 1999). With respect to ensemble methods, they avoid carrying along an ensemble of model runs that generally makes the system too expensive; therefore, they have the advantage of computational efficiency, and can be tuned by adjusting one or more parameters, such as the error correlation length scale. For example, Kuang et al. (2009) use a simple  $\mathbf{P}^f$

$$P_{ij}^f = \rho_i \sigma^2 \delta_{ij}, \tag{24}$$

in which

$$\rho_i = \frac{(r_i - r_c)^2}{(r_{do} - r_c)^2} [3(r_{do} - r_c) - 2(r_i - r_c)] \left(1 - \frac{r_i - r_{do}}{r_{do}}\right) \quad \text{for } r_i \geq r_c, \tag{25}$$

where  $r_i$  denotes the  $i$ -th radial grid point,  $r_{do}$  is the mean radius of the top of the  $D''$ -layer,  $r_c$  is the correlation distance from the CMB, and  $\sigma$  is a constant forecast error standard deviation. One could optimize the analysis by changing the correlation length  $r_c$ . For the detailed mathematics, we refer the reader to Kuang et al. (2009).

This modelling approach has been incorporated in a series of observing system simulation experiments (OSSEs), in which a model run is used as the true state of the system,  $\mathbf{x}'$  (generally referred to as a nature run) (Liu et al. 2007). From this nature run, observations are generated using the observation operator with added observation error using (4). The assimilation system then uses these synthetic observations with another model run, generally with somewhat different parameter values. OSSEs are used to determine the impact of the assimilation on the unobserved state of a system, which for the geodynamo is nearly the entire state. These experiments therefore have the potential to show whether geomagnetic data assimilation has any potential to really improve our estimates of the dynamics of the Earth’s core.

An example of this potential is seen in Fig. 9, which shows the radial component  $u_r$  of velocity  $\mathbf{u}$  at a distance of 35 km below the CMB for three different cases. A nature run with parameter values  $R_{th} = 15000$ ,  $Ro = 1.25 \times 10^{-6}$  and  $E = 1.25 \times 10^{-6}$  is shown in panel (a). Panel (b) shows  $u_r$  from a free model run with the same parameter values except  $R_{th} = 14500$  while panel (c) shows  $u_r$  after running the assimilation for a time of  $0.892 \tau_d$ , where  $\tau_d$  is the Earth’s magnetic free decay time. Observations of the poloidal magnetic field at the CMB from the nature run with degree  $l \leq 8$ , are assimilated into the model every  $0.01 \tau_d$ . The results show that the assimilation results in a measurable improvement in the radial velocity at this location. In other words, corrections to the poloidal magnetic field will in turn influence the other state variables through the model simulation. Thus, this univariate assimilation of geomagnetic data could be seen to improve the estimation of fluid motion in the Earth’s outer core.

Kuang et al. (2009) have applied this system with the surface geomagnetic measurements over the past 100 years. In this application, analysis is made every 5 years. The rms error  $\epsilon$  is defined as

$$\epsilon = \left\{ \frac{1}{A} \int \left[ (\tilde{b}_r^f) - (\tilde{b}_r^o) \right]^2 dA \right\}^{1/2}, \tag{26}$$

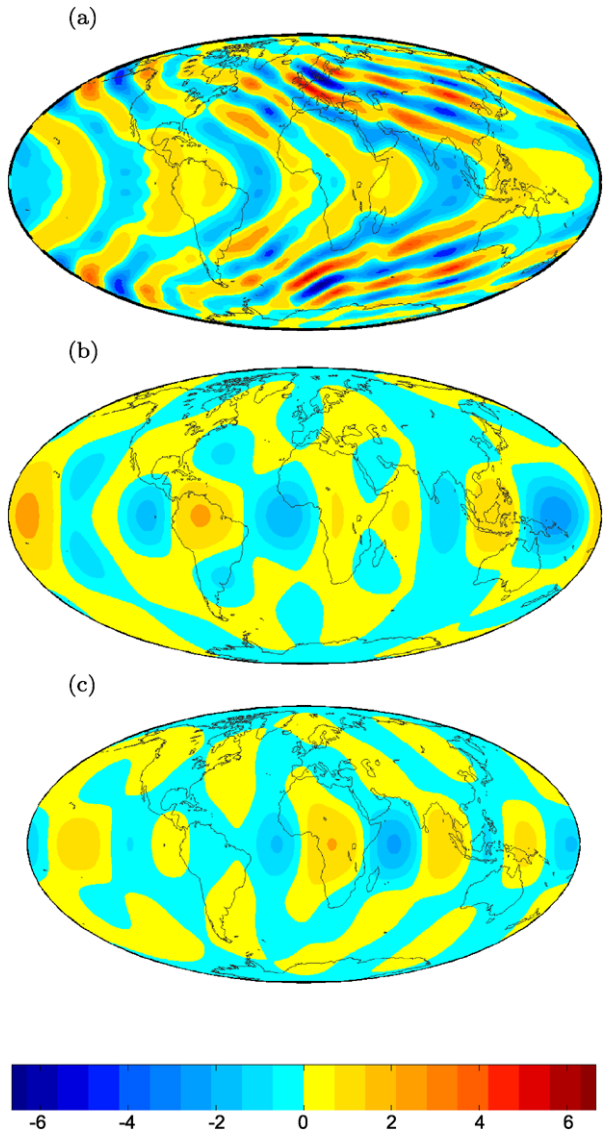
where the superscripts  $f$  and  $o$  have their usual meaning, and  $\tilde{b}_r$  is related to the spherical harmonic coefficients  $b_l^m$  of the poloidal field at the top of the  $D''$ -layer (whose surface is denoted by  $A$ ) by

$$\tilde{b}_r = \sum_{0 \leq m \leq l} \frac{l(l+1)}{r^2} \left( \frac{b_l^m}{b_1^0} \right). \tag{27}$$

As shown in Fig. 10, the errors between the assimilated results and surface geomagnetic observations decrease over time, i.e. the model outputs are drawn closer to the observations. The reduction of the errors could be attributed to the changes of the state variables inside the core (Kuang et al. 2009). But since this assimilation is using real observations, there is no known ‘true’ state with which to compare the changes to the unobserved state variables. However, we can plot the differences in the core state between model runs with and without assimilation. For example, Fig. 11 shows the relative change in the toroidal magnetic field over the one hundred year assimilation run, which reaches as much as 40%. The improved poloidal magnetic field forecast is an indication that these changes have resulted in an improved estimate of the toroidal magnetic field.

In fact, it is worth noting that such geomagnetic data assimilation schemes are already tentatively used in geomagnetic field modeling for short-term forecasting purposes. Indeed, Kuang et al. (2010) utilizes 7,000 years of the field models derived from pale-

**Fig. 9** Radial velocity,  $u_r$ , on a spherical shell 35 km below the CMB from a nature run (a), a free model run (b) and the forecast after assimilating observations from the nature run with  $l \leq 8$  (c). Assimilation was done every 20 years for 17840 years. The velocities in each panel are non-dimensional (common color scale at the bottom). A non-dimensional velocity of unity implies  $1.75 \times 10^{-2}$  km/y



omagnetic, archeomagnetic, historical magnetic, observatory and satellite magnetic data in their geomagnetic data assimilation system (MoSST\_DAS). In addition, a prediction-correction algorithm is used to reduce the dynamo system model errors in assimilation output. Their forecasts are benchmarked with earlier forecasts, in particular those of IGRF-8 and IGRF-9. The results demonstrate that, their 5-year field forecasts are comparable to IGRF, and their 5-year SV forecasts are more accurate (with smaller misfit). Using the same system, and the field model output up to 2010, they produced a 5-year SV forecast for the period from 2010–2015. Their forecast is now a component of IGRF-11.

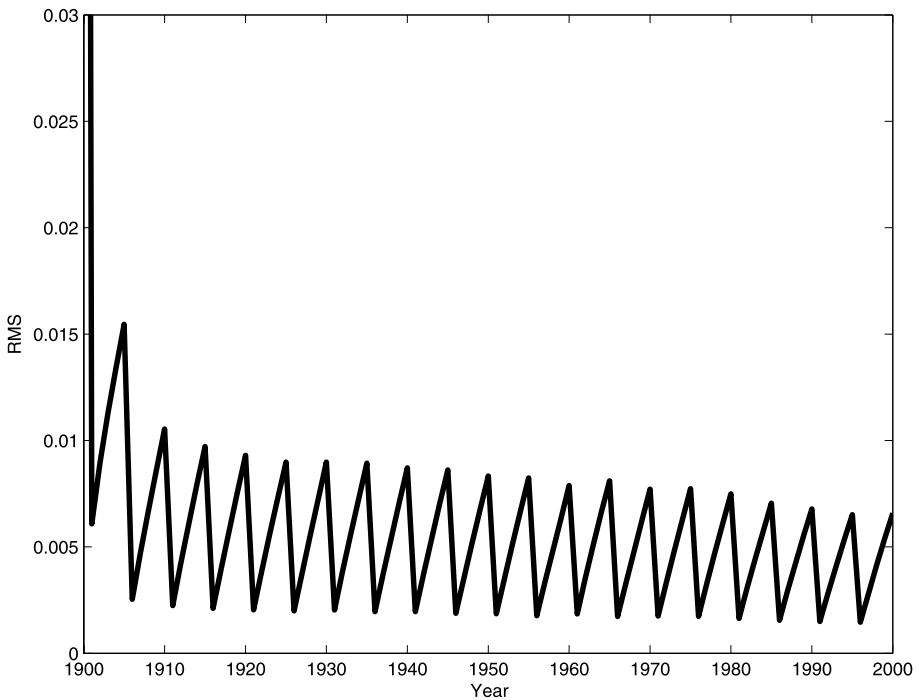


**Fig. 10** The difference between the poloidal field at the DDB inverted from surface geomagnetic observations and that from assimilation during the past 100 years. The analysis time, i.e. the time interval between two adjacent analyses, is 5 years

#### 4.2 Variational Assimilation Based on Models Tailored to Account for Observations of the Secular Variation

Following an alternative route, Canet et al. (2009) decided to develop a minimal model of core dynamics  $M$  able to account for the observed secular variation. They resort to a quasi-geostrophic approach which aims at describing core processes on short time scales (years to decades). Viscous forces can be readily neglected outside boundary layers and detached shear layers, provided those localized regions do not exert a control on the main body of the fluid. Canet et al. (2009) therefore followed the common practice of defining the core surface flow  $\mathbf{u}_h$ , which appears in (1), as the flow beneath the viscous Ekman layer attached to the core-mantle boundary.

Three-dimensional simulations of the geodynamo (as governed by (21)–(23)), if performed at very low Ekman number ( $E \approx 5 \times 10^{-7}$ ), require formidable computational power; even if data that can be assimilated are available for no more than a small fraction of a magnetic diffusion time, these simulations are currently out of reach for data assimilation practice in that region of parameter space.<sup>12</sup> Interestingly, though, these recent high-resolution simulations have yielded Earth-like ratios of the magnetic to kinetic energy

<sup>12</sup>An assimilation scheme requires good model error statistics. Even if one resorts to a frozen background error covariance matrix (the optimal interpolation approach to sequential data assimilation), the estimation of that matrix demands to run the model over a significant amount of time (several magnetic diffusion times), which becomes prohibitive in the parameter range recently explored by e.g. Sakuraba and Roberts (2009).

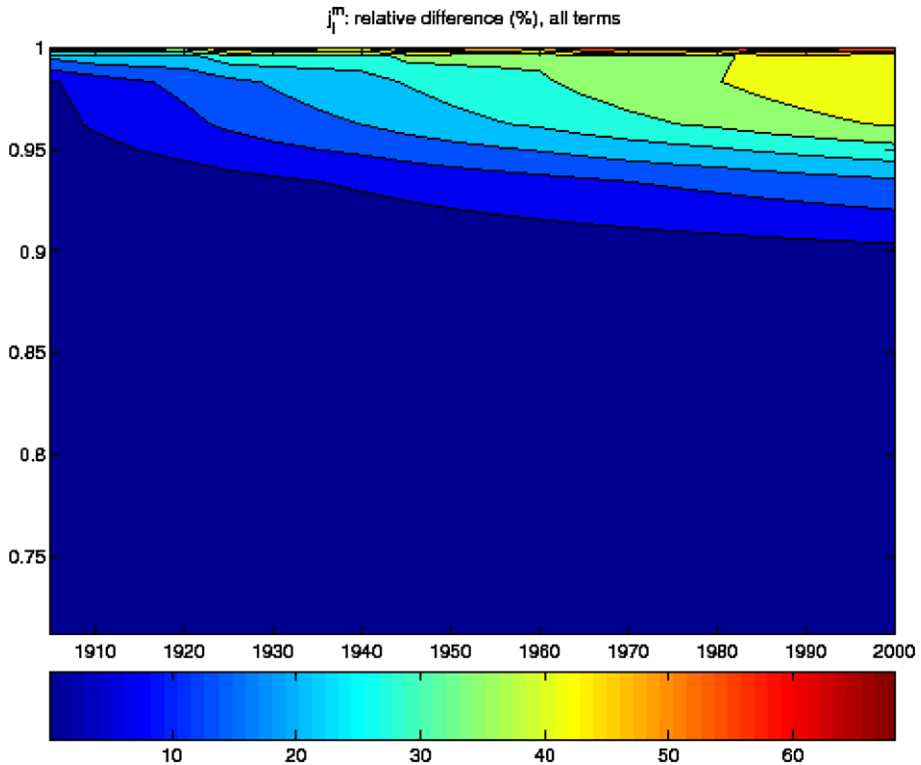


**Fig. 11** The relative difference in toroidal magnetic field between the forecast from the assimilation run and the free running model, as a function of time ( $x$ -axis) and radial position ( $y$ -axis). The analysis is calculated every 20 years (1900, 1920, 1940, 1960 and 1980). The color scale is in percent

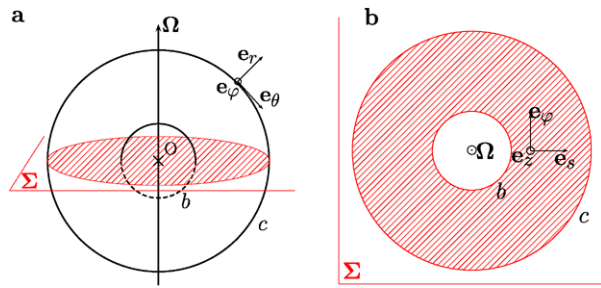
for the largest length scales (Takahashi et al. 2008; Sakuraba and Roberts 2009). For a small enough magnetic Prandtl number  $Pm$  (typically 0.2), they exhibit smaller scale convection vortices as the Ekman number is decreased towards Earth-like values, while not much variation in the dominant scale of the magnetic field is observed. These simulations thus give hints of dynamo generation taking place at length scales that are kept out of view of the myopic observer at the Earth's surface. That behaviour prompted Canet et al. (2009) to investigate a model which involves only the velocity and magnetic fields, leaving aside the buoyancy forces which power the geodynamo and are responsible for changes in the magnetic field occurring on long (millennial, say) time scales.

On the shorter secular variation time scales, rotation forces are much larger than magnetic forces in the bulk of the fluid. On the basis of theoretical arguments and numerical calculations, Jault (2008) argued that rapidly rotating motions of length scale  $\mathcal{L}$  are axially

---

In addition, ensemble covariances in sequential algorithms increase the assimilation runs at least by one order of magnitude (the size of the ensemble), thus effectively increasing simulation time well beyond a free magnetic decay time. Similar conclusions apply to variational assimilation algorithms: The background error covariance matrix entering the definition of the cost function (16) is the same as the one used in an optimal interpolation framework (its proper determination is therefore as costly). In addition, the minimization of the objective function requires several tens of iterations, since it is not conceivable to come up with a direct estimate of the Hessian.

**Fig. 12** Geometry of the system and notations used to describe the quasi-geostrophic model of core dynamics. **(a)** Side view. **(b)** Equatorial section.  $\Sigma$  is the equatorial plane, while the CMB corresponds to the outer sphere, located at  $r = c$ ;  $b$  is the radius of the inner core. Modified after Canet et al. (2009)



invariant if the relevant non-dimensional Lehnert number,  $Le$ , is small enough. That number measures the ratio between the period of inertial waves,  $1/\Omega$ , and the period of Alfvén waves,  $T_A = \mathcal{L}/V_A$  (Lehnert 1954):

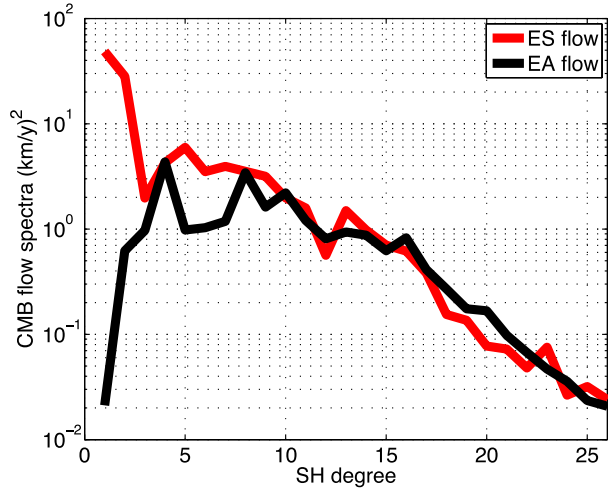
$$Le = \frac{B_0}{\Omega(\mu\rho)^{1/2}\mathcal{L}}. \tag{28}$$

The Alfvén wave speed  $V_A$  is classically defined as  $V_A = B_0/\sqrt{\rho\mu}$ ; note that  $Le$  is a decreasing function of the length scale  $\mathcal{L}$ . In the series of calculations carried out by Jault (2008), the flow appears to be invariant in the direction parallel to the rotation axis, provided  $Le \ll 1$ . For the Earth’s core, a magnetic field strength  $B_0$  on the order of 2 mT (Christensen et al. 2009) and a scale  $\mathcal{L}$  of 1,000 km yield  $Le \approx 10^{-4}$ , well below unity. Therefore, Canet et al. (2009) assume that the high frequency Earth’s core flows, responsible for the observed geomagnetic secular variation, are geostrophic at leading order. Instead of  $Le$ , which is based on the magnetic field intensity  $B_0$  and a characteristic length scale  $\mathcal{L}$ , the appropriate small parameter to characterize the approximation is related to the slopes of the spherical boundaries (e.g. Gillet et al. 2007, and references therein). Indeed, motions with a non zero component in the cylindrical radial direction cannot be fully geostrophic in a spherical shell. Working in the equatorial plane  $\Sigma$  (crosshatched in Fig. 12), a cylindrical set of coordinates  $(s, \varphi, z)$ , with  $e_z$  parallel to the axis of rotation, is well-suited to study the resulting columnar patterns. The  $s$  and  $\varphi$  components of the velocity are independent of  $z$ . Outside the cylindrical surface parallel to the rotation axis and tangent to the inner core (the so-called tangent cylinder), the  $z$  component of the velocity  $u_z$  varies linearly with  $z$ , in order for the total flow  $\mathbf{u}$  to satisfy the no-penetration condition at the outer boundary. Inside the tangent cylinder, one can write  $u_z = a(s) + b(s)z$ , and choose properly the two functions  $a$  and  $b$  which guarantee that the total flow satisfies the no-penetration condition at both the ICB and the CMB. Outside the tangent cylinder, the quasi-geostrophic flow is uniquely defined by its streamfunction  $\psi$  in the equatorial plane.

The quasi-geostrophic assumption is somehow supported by inversions of tangentially geostrophic core surface flows  $\mathbf{u}_h$ , which do not assume equatorial symmetry. Figure 13 shows the spectrum of the kinetic energy at the core surface as a function of spherical harmonic degree  $l$ , after separating  $\mathbf{u}_h$  into its equatorially symmetric (ES) and equatorially antisymmetric (EA) components (the red and black curves, respectively). The ES component appears to be stronger than the EA component at the largest scales, at least up to  $l = 7$ .

Using the two-dimensional framework outlined above, the calculation of core surface flows is then incorporated inside a prognostic dynamical model which describes the time evolution of the corresponding streamfunction  $\psi$ . Retaining the Lorentz forces for the reasons outlined above implies averaging the magnetic contribution to the vorticity equation along the direction of rotation of the Earth, following a procedure akin to that of Hide

**Fig. 13** Spectrum of the energy of the core surface flow inferred from the model xCHAOS of Olsen and Manda (2008) divided into its equatorially symmetric (ES, red curve) and antisymmetric (EA, black curve) components. The calculated core flow  $u_h$  has been obtained over the time interval [2000–2007] after ensemble averaging 10 different solutions obtained using 10 different realizations of the invisible small-scale magnetic field (spherical harmonic degree  $l \geq 13$ ). Consult Gillet et al. (2009) for further details on the method



(1966), who worked in the  $\beta$ -plane. This yields a term involving only quadratic products of the equatorial components of the magnetic field  $B_s$  and  $B_\phi$ , namely  $B_s^2$ ,  $B_s B_\phi$  and  $B_\phi^2$  (Canet et al. 2009). We shall use the generic notation  $B^2$  to refer to these quantities. The induction equation in the core interior can also be transformed into an equation for the evolution of  $B^2$ . Coupling the axial vorticity equation and this modified induction equation, we obtain an extension to non axi-symmetrical core flows of the torsional oscillation model of Braginsky (1970), which involved only

$$\{B^2\}(s) = \frac{1}{2h(s)} \frac{1}{2\pi} \int_0^{2\pi} \int_{-h(s)}^{h(s)} B_s^2(s, \varphi, z) dz d\varphi, \tag{29}$$

in which  $h(s)$  is the half-height of the geostrophic cylinder of radius  $s$ . At the core surface, the flow interacts with the magnetic field, through the radial component of the magnetic induction equation. That part of the model connects the dynamics and the observed secular variation, with the radial component of the magnetic field acting as a passive tracer. In summary, the state of the Earth’s core in that approach consists of  $B_r$  at the core surface, together with the equatorial streamfunction  $\psi(s, \varphi)$  and quadratic quantities  $B^2(s, \varphi)$ .

Omission of buoyancy in this model can be challenged. Indeed, Amit et al. (2008) and Aubert et al. (2008) have recently suggested an alternative or complementary model as they have investigated steady core surface flow driven by thermal coupling with the heterogeneous lower mantle. As the mantle and the solid inner core evolve on very long time scales, thermal coupling with heterogeneous solid boundaries can be the source of significant steady flows (Aubert et al. 2007), but not of the rapidly changing flows, of the kind inferred from the recent secular variation observed from satellites (Olsen and Manda 2008).

From the methodological standpoint, Canet et al. (2009) resort to variational data assimilation to construct formally the relationship between model predictions and observations, following the 4D-Var approach described in Sect. 2.2.2. They have investigated the effect of several factors on the solution (width of the assimilation time window  $T$ , amount and quality of data), and they have discussed the potential of the model to deal with real geomagnetic observations. They have illustrated that framework with twin experiments, performed first in the case of the kinematic core flow inverse problem, and then in the case of Alfvén torsional oscillations. In both cases, using the adjoint model enables the estimation of core



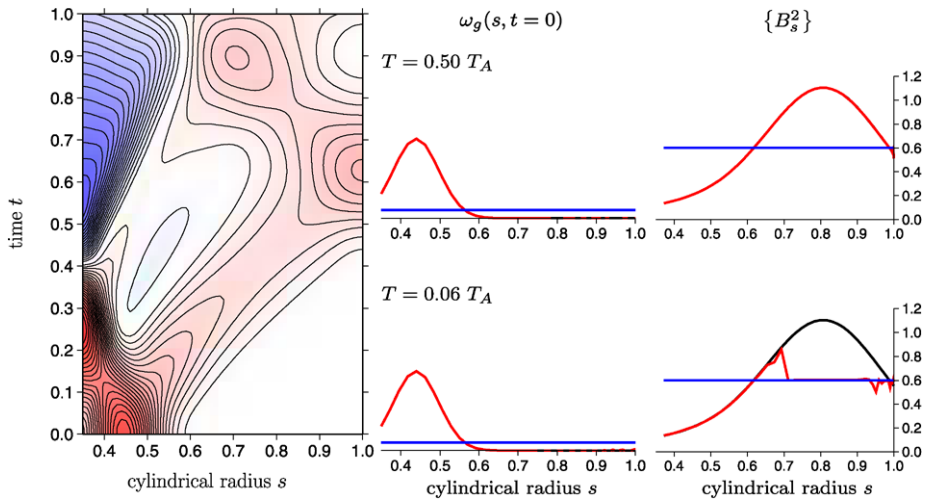


**Fig. 14** Torsional oscillations twin experiments in a 4D-Var framework. The control vector for these experiments consists of the initial angular velocity profile in the core,  $\omega_g(s, t = 0)$ , along with the profile of the static magnetic quantity  $\{B_s^2\}(s)$ . *Left*: cylindrical radius-time plot of  $\omega_g$  showing the propagation of a synthetic, reference torsional wave in the region outside the tangent cylinder (cylindrical radius  $b < s < c$ ). *Red* is positive, *blue* is negative (absolute scale is arbitrary). Length and time are scaled by  $c$  and  $T_A$ , respectively. With our choice of scales, an Alfvén time amounts to 6 y. *Center and right panels*: Assimilation results, for two widths of the time interval over which assimilation has been carried out:  $0.5 T_A$  (top row) and  $0.06 T_A$  (bottom row). *Center panel*: the initial angular velocity profile  $\omega_g(s, t = 0)$ . In *black*: the true profile. In *blue*: the initial guess. In *red*: the result obtained after assimilation. *Right panel*: same for  $\{B_s^2\}(s)$ , which is plotted in units of  $B_0$ , i.e. 2 mT. Note that in most instances, the *red* and *black* curves are superimposed

state variables which, while taking part in the dynamics, are not directly sampled at the core surface. A pedagogical example of such a behaviour is provided in Fig. 14: The reference (true) case consists of an initial perturbation of the angular velocity (with respect to a solid-body rotation),  $\omega_g^t(s, t = 0)$ , which propagates in the outer core with a local wavespeed proportional to the rms value of  $B_s$  over a geostrophic cylinder (defined in (29)). That progressive torsional wave interacts with  $B_r$  at the core surface to generate a synthetic database of secular variation,  $\partial_t B_r^t$ , over a time interval of width  $T$ , assuming an error-free measurement ( $\epsilon^o = \mathbf{0}$ ). Assuming next a wrong initial condition for  $\omega_g$  and an incorrect profile for  $\{B_s^2\}$ , the adjoint model can be used in conjunction with the database to correct the guesses for  $\omega_g(s, t = 0)$  and  $\{B_s^2\}(s)$ . In Fig. 14, the results obtained after assimilating the perfect synthetic observations are shown for two values of  $T$ , corresponding to a short and a long window (spanning 6% and 50% of an Alfvén time, respectively). In both cases, the retrieval of  $\omega_g(s, t = 0)^t$  is perfect in that noise-free context (because the secular variation is directly sensitive to the initial condition), whereas the retrieval of  $\{B_s^2\}^t$  is only achieved over the portion of the domain which has been effectively sampled by the wave during its propagation. The short interval case is indeed characterized by a shadow zone which covers the outer third (in radius) of the outer core (see the bottom right panel in Fig. 14); that zone has been illuminated by the passing of the wave in the longer time interval case.

The history of the determination of the magnetic field within the core from the study of torsional oscillations gives us a note of caution about the use of simplified models. It shows that, unfortunately, the choice of the model can dictate the answer. Braginsky (1970, 1984) argued that both LOD variations and magnetic field records show oscillations with periods



about 60 years. If we identify that period with the period of the fundamental eigenmode for torsional oscillations, we obtain an estimate for the rms  $s$ -component of the magnetic field within the core  $B_s \approx 0.2$  mT. However, the same model can be used to account for variations with periods of about 6 years (Gillet et al. 2010a). Then, we obtain  $B_s \approx 2$  mT. In that latter case, we can associate the longer period variations with non-zonal fluctuations which drive the zonal circulation. Both models can nevertheless provide an adequate fit to the data, because the uncertainties on the flow coefficients are very large (Buffett et al. 2009).

From the discussion of this example, we can emphasize two points. First, a good grasp of the different error sources is crucial. As outlined in the introduction, the difficulties arising because of the invisible small scale magnetic field at the core-mantle boundary are now well identified (Eymin and Hulot 2005). They translate into uncertainties in the coefficients of  $\psi$  (errors of representativeness) that can be accurately estimated using an ensemble technique (Gillet et al. 2009). Second, the transfer of data assimilation methods to the geomagnetic community has been slowed down by our poor knowledge of the state of the Earth's core prior to the assimilation of geomagnetic data.

That remark calls for an incremental approach whereby our knowledge of the state of the Earth's core  $\mathbf{x}$  progressively improves. As noted above (Sect. 1.1), we arguably have a good knowledge of the largest scales of the quasi-geostrophic streamfunction  $\psi$  time-averaged over the last ten years during which highly accurate satellite data have been available. On the other hand, time series of  $\psi$  inferred from continuous magnetic field models such as CM4 (Sabaka et al. 2004) for the time interval 1960–2002 show artifactual variations. This situation has prompted different groups to forgo sequential approaches and undertake simultaneous predictions of  $B_r$  and of the flow (or the streamfunction  $\psi$ ) at the core surface (Lesur et al. 2010). We can look at these efforts as a step preliminary to the use of the full QG scheme outlined in this section.

### 4.3 Core Field Forecasting and Earth's Dynamo Limit of Predictability

In parallel to the efforts reported above, which mainly focussed on the ability of data assimilation schemes to recover some information about the hidden components of the state of the geodynamo (such as the magnetic field deep inside the core, recall Figs. 11 and 14), a number of studies have also started looking into the possibility of improving geomagnetic (core) field forecasts. Such forecasts are not only of academic interest. They are very much needed to ensure that an accurate enough global model of the geomagnetic field is permanently available for a large number of practical applications such as navigation, pointing (e.g. for directional drilling), pre-processing of local magnetic surveys for exploration geophysics, and defining the magnetic environment in the near outer space for ionospheric, magnetospheric, and space weather applications (see e.g. Meyers and Davis 1990, for an interesting account of those many, sometimes unexpected, applications). Most of those needs are currently covered by the International Geomagnetic Reference Field (IGRF) models, which are updated, published and widely distributed every five years (see e.g. Maus et al. 2005). Those models are conventionally provided in the form of a set of Gauss coefficients (up to degree 13) defining a spherical harmonic description of the field at a reference epoch (the latest IGRF has just been released for reference epoch 2010.0),<sup>13</sup> together with an additional set of estimates of the first time derivative of those coefficients (up to degree 8), to be used for forecasting the field over the next five years. Thus IGRF forecasts basically rely on a simple linear extrapolation of the field in time.

<sup>13</sup>[www.ngdc.noaa.gov/AGA/vmod/igrf.html](http://www.ngdc.noaa.gov/AGA/vmod/igrf.html).

For most applications, increasing the range of the forecast beyond five years is less an issue than improving the accuracy of the forecast. For other applications, however, increasing the range of the forecast is very much desirable. It is well-known for instance that the global intensity of the field is currently decreasing, especially within a wide region in the South-Atlantic where the field is already much lower than anywhere else, defining a so-called South-Atlantic Anomaly (SAA, see e.g. Hulot et al. 2007). This anomaly evolves very significantly on decadal time scales (e.g. Olsen et al. 2000), through core processes that could lead to a further decrease of the field in this area (Hulot et al. 2002). As the SAA is already an issue to low Earth orbiting space technology (e.g. Heitzler 2002), which requires significant time for planning and operation, improving our ability to forecast the evolution of the field up to several decades would unquestionably be valuable.

Studies investigating how geomagnetic field forecasting could be improved (compared to the linear IGRF five-year range type of forecasting) have been very few so far. A first series of studies, illustrated by the two recent papers of Maus et al. (2008) and Beggan and Whaler (2009), looked into the possibility of relying on the initial value problem described by (1) to forecast the field. Starting from an initial field  $B_r$  at time  $t_0$  and assuming a flow  $\mathbf{u}_h$  known over the forecasting time window, (1) can be time stepped, and the trajectory of  $B_r$  computed, over the same window. Since, as already noted in Sect. 3, knowing  $B_r$  at the core surface is equivalent to knowing the field at the Earth's surface and above (where we are interested in predicting the core field), this makes it possible to forecast the field. Note that this forecasting strategy is indeed different from the IGRF strategy: Following the latter would imply to start as well from a known  $B_r$  at  $t_0$ , but to use a steady right-hand side term (equal to  $\partial_t B_r$  at  $t_0$ ), when time stepping equation (1). In particular, even assuming a forecast based on a stationary flow  $\mathbf{u}_h$  is different from an IGRF forecast, as the field  $B_r$  in the right-hand side term of (1) evolves at each time step, making this term time-dependent.

Using such a core flow based forecasting strategy is a natural first step towards improving on the trivial IGRF forecasting strategy. It nevertheless relies on two fundamental assumptions that need to be spelled out. One is that magnetic diffusion is not expected to play any significant role on the time and length scales of interest. This indeed is widely thought to likely be the case (see e.g. Jackson and Finlay 2007; Holme 2007). The other, far less grounded, is that better a priori information is available with respect to the flow  $\mathbf{u}_h$  and its time behaviour, than with respect to the field  $B_r$ . This is a strong assumption, especially in view of the dynamical interplay between the magnetic field and the flow expected within the quasi-geostrophic conceptual framework discussed in Sect. 4.2. However, and as already pointed out, it may also be that some background quasi-stationary core flows driven by mantle thermal heterogeneities could play a significant role, especially when considering long time scales (Aubert et al. 2007, 2008; Amit et al. 2008). Interestingly, Maus et al. (2008) precisely suggest that using a stationary flow  $\mathbf{u}_h$  could slightly improve the quality of the forecast when considering predictions up to a decade, beyond the time scale of short term dynamics associated with the so-called geomagnetic jerks. The still unpredictable occurrence of these remains the main limitation to short-term forecasting (see e.g. Thébaud et al. 2010). Although such simple core flow based geomagnetic field forecasts are much debated (e.g. Lesur and Wardinski 2009; Maus et al. 2009), further developments, associated with data assimilation techniques, such as initiated by Beggan and Whaler (2009), and with physical models, along the lines discussed in Sects. 4.1 and 4.2, are clearly the way to additional improvements.

An interesting question to be discussed at this point is that of the limit of predictability of the Earth's dynamo. Just as for meteorology, any geomagnetic field forecast is indeed intrinsically limited in time. This is because the geodynamo belongs to the same class of

non-periodic dynamical systems that can exhibit chaotic behaviour. As first pointed out by Edward N. Lorenz in his celebrated 1963 paper (Lorenz 1963), for such systems, unless the initial state is perfectly known, future states are bound to become unpredictable after a finite period of time, even if computed from exactly known deterministic equations. This is because any initial error with respect to the true state of the system  $\mathbf{x}^t$ , no matter how small, will necessarily grow at some exponential rate and eventually lead to a predicted state  $\mathbf{x}^f$  macroscopically different from  $\mathbf{x}^t$ . In the case of the atmosphere, it is for instance estimated that any initial error will roughly double within 1.5 days (Kalnay 2003), which, given current meteorological data quality and assimilation strategies, translates into the familiar possibility of accurately forecasting the weather up to three days in advance (recall Sect. 1.2), with some confidence up to a week, but hardly beyond. Although some attempts have been made early on to characterize the non-linear behaviour of the Earth's dynamo by using simplified equations (e.g. Jones et al. 1985), it is only very recently that the issue of the associated limit of predictability has begun to be addressed with the help of fully consistent 3D magnetohydrodynamic codes, of the same type as those envisioned for the data assimilation approach described in Sect. 4.1.

The first study of this type has already provided interesting results (Hulot et al. 2010a). It consisted in a systematic study of a series of numerical dynamo simulations, the dynamo being assumed thermally driven with fixed and homogeneous temperatures imposed at both the inner-core and core-mantle boundaries, with the electrically conducting inner core (with the same conductivity as the liquid core) free to rotate axially (along the Earth's rotation axis) with respect to the electrically insulating mantle, and the mechanical boundary conditions assumed rigid at both boundaries. Although such assumptions can be considered as quite restrictive (in particular because internal heat sources, and compositional sources are ignored), they have several advantages. First, they are typical of the type of assumptions currently used for initial attempts of implementation of data assimilation strategies with three-dimensional models of the geodynamo (see Sect. 4.1 above). Second, they make it possible to run a large number of simulations under well-understood physical assumptions, with each simulation characterized by four input dimensionless parameters (the Rayleigh  $R_{th}$ , Ekman  $E$ , Prandtl  $Pr$ , and magnetic Prandtl  $Pm$  numbers, see Table 3). Finally, and as precisely suggested by the study of Hulot et al. (2010a), it anyway seems that the issue of the limit of predictability of fully consistent 3D dynamos is less dependent on the details of the way the dynamo is driven, than on the constitutive dimensionless parameters  $E$ ,  $Pr$ , and  $Pm$ , the output parameter  $Rm$  (the magnetic Reynolds number, see Table 3), or the typical correlation times of the field produced at the core surface, estimates of which can be derived from both contemporary and archeomagnetic observations (Hulot and Le Mouél 1994; Hongre et al. 1998). Thanks to the relatively large number of simulations they ran (37 in total), Hulot et al. (2010a) were thus able to investigate the dependence of the limit of predictability of such dynamos on those various parameters, and propose a relatively simple asymptotic rule that they tentatively applied to the Earth's dynamo.

To both illustrate the origin of this limit of predictability and the method used by Hulot et al. (2010a) in their investigation, Fig. 15 shows the consequence of artificially introducing a slight error in one such simulation. In this figure, we first show the time evolution of the axial dipole field produced at the core surface by the reference simulation (Fig. 15a), which experienced a reversal. This reference simulation was next slightly perturbed by adding an error of relative value  $\epsilon$  to the axial dipole at a given time  $t_0$  (here close to the reversal). The consequence of introducing this perturbation in the subsequent evolution of the simulation is next shown in Fig. 15b, where a close-up of the initial dipole evolution is plotted, together with the dipole evolution after introducing relative errors of  $\epsilon = 10^{-2}$ ,  $\epsilon = 10^{-6}$ ,

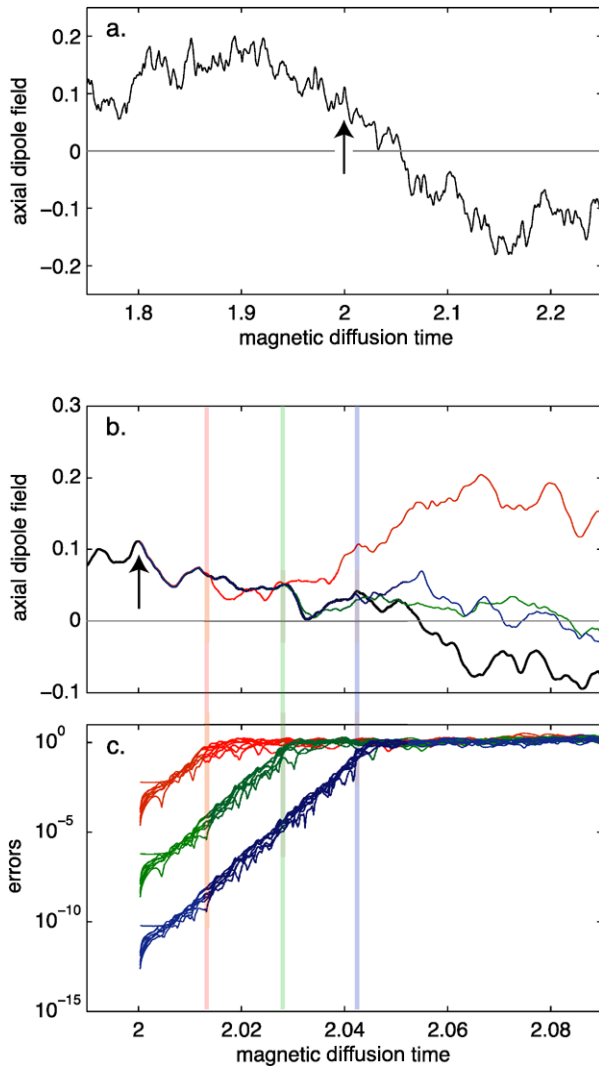


**Fig. 15** Error growth in a perturbed fully consistent 3D dynamo simulation, with  $E = 4 \times 10^{-4}$ ,  $Pr = 1$ ,  $Pm = 10$  and  $Rm \approx 770$ , following the definitions given in Table 3, which are slightly different from those chosen by Hulot et al. (2010a). In (a) we first show the evolution of the axial dipole field at the core surface (arbitrary scale) for a reference run as a function of time (scaled in units of magnetic diffusion time  $\tau_D = d^2/\lambda$ ,  $d$  being the depth of the core, see Table 3). At time  $t_0 = 2.00$  (arrow), perturbations with various magnitudes are introduced and the subsequent evolution of the axial dipole field of the perturbed solutions are shown in (b) ( $\epsilon = 10^{-2}$  red,  $\epsilon = 10^{-6}$  green, and  $\epsilon = 10^{-10}$  blue), which also shows a close-up of the reference solution (black). The detailed way those various perturbed solutions diverge from the reference solution are finally shown in (c), which shows semi-logarithmic plots of the relative rms differences for each spherical harmonic degree  $l$  (with  $1 \leq l \leq 8$ , leading to eight overlapping curves) between the core surface poloidal magnetic field produced by the reference simulation and that produced by each perturbed solution (same colour-code as for (b)). Colour-coded vertical bars mark the times when the perturbed solutions start behaving in a way totally unrelated to the reference solution (consult Hulot et al. 2010a for more illustrations and details)

and  $\epsilon = 10^{-10}$ . As can be seen, the perturbed solutions first remain very close to the reference solution, but eventually diverge macroscopically from this solution. The larger the initial error, the sooner the divergence occurs. As shown in Fig. 15c, this is because the difference between the perturbed solution and the reference solution (e.g., the error) gradually increases in an exponential manner with a growth rate independent of the initial error  $\epsilon$ . The same growth rate is found in the way all quantities defining the state of the dynamo  $\mathbf{x}$  diverge from their evolution in the reference simulation (such as the higher degrees of the poloidal magnetic field at the core surface, as plotted in Fig. 15c). As shown by Hulot et al. (2010a) it also is independent of the way and time  $t_0$  (including shortly before a reversal, as is the case here) the perturbation is initially introduced (be it in the magnetic, flow, or temperature fields). Thus, this error growth rate appears to be an intrinsic property of each given dynamo. It can be defined as  $\lambda_e = \tau_e^{-1}$ , where  $\tau_e$  is the associated  $e$ -folding time. This  $e$ -folding time of course depends on the dimensionless parameters governing the dynamo simulation under consideration. But as noted by Hulot et al. (2010a), and at least for the parameter range they investigated, as soon as the magnetic Reynolds number  $Rm$  produced by the dynamo is large enough, and even more so when considering E, Pr, and Pm parameter ranges closest (though still very remote, see below) to those thought relevant for the geodynamo, it appears that  $\tau_e$  only depends on a time scale  $\tau_{sv}$  that statistically characterizes the time variations of the field produced at the core surface, roughly as

$$\tau_e = 0.05\tau_{sv}. \quad (30)$$

The time scale  $\tau_{sv}$  can be recovered from observations by inspection of the spatial power spectra of the field and of its first time derivative (see Hulot and Le Mouél 1994; Christensen and Tilgner 2004; Hulot et al. 2010a, for details). For the geodynamo,  $\tau_{sv}$  turns out to be of order 535 years (Christensen and Tilgner 2004). Thus, the study of Hulot et al. (2010a) would suggest a value of about 30 years for  $\tau_e$ , amounting to a doubling time of roughly 20 years, analogue of the 1.5 days doubling time in meteorology.

Assessing how far in the future the core field could then be forecasted (that is, assessing the practical limit of predictability of the Earth's dynamo) also requires some consideration on how well the state of the geodynamo  $\mathbf{x}$  could possibly be known at some initial time. This is clearly not a trivial issue. Given the current status of data assimilation schemes, it is fair to say that at present, many of the quantities that define  $\mathbf{x}$  are poorly known (particularly those defining the state of the field and flow deep inside the core). As the methods described in Sects. 4.1 and 4.2 improve, it is not unreasonable to expect some significant progress in the coming years. But it also is clear that the basic state of the geodynamo will never be known with better accuracy than the core field that can directly be observed at the Earth's surface. As already noted in Sect. 3, this accuracy is intrinsically limited by the crustal field, which does not make it possible to recover the static component of the core field beyond spherical harmonic degree 14, and its time variations beyond degree 18. In addition, in practice, even those degrees of the core field that can be recovered in principle are only recovered with some uncertainties. Using the order of magnitude of the error associated with current IGRF models (typically of order 10–20 nT at the Earth's surface at the epoch of reference of the model, the average magnitude of the field being of order 40,000 nT), and the fact that current linear IGRF type of forecasts lead to errors typically of order 100 nT after just 5 years, Hulot et al. (2010a) note that the above results would suggest that using an ideal assimilation scheme could possibly lead to a prediction of similar quality after 50 to 70 years, thus leaving some room for significant improvements compared to the current simple IGRF linear forecasts.

Probably the main limitation of the Hulot et al. (2010a) investigation is the parameter regimes in which the simulations operate, which are still very remote from the one thought to be relevant for the geodynamo (with  $E = 10^{-3}$ – $10^{-5}$ ,  $Pr = 1$ , and  $Pm = 0.5$ – $15$ , whereas  $E = 10^{-9}$ – $10^{-14}$ ,  $Pr = 0.1$ – $1$ , and  $Pm = 10^{-5}$ – $10^{-6}$  are thought to be appropriate for the Earth). In this respect, extrapolating the asymptotic rule given by (30) to the Earth can be considered as a strong move. However there is far less doubt that those results essentially apply to all fully consistent 3D numerical dynamos that could be used in practice for data assimilation. Since those would have to produce a field with the same  $\tau_{sv}$  time scale as the geodynamo and be fed by the observed field with the same initial error as described above, forecasts based on such 3D dynamos would then indeed be limited by the limit of predictability identified by Hulot et al. (2010a). Unfortunately, additional limitations could then also arise as a result of the fact, already mentioned (see Sect. 1.3), that all such 3D dynamos tend to damp out high frequency magnetohydrodynamic phenomena such as torsional oscillations and geomagnetic jerks (both of which could be related, see e.g. Bloxham et al. 2002). Interestingly however, we also note that such phenomena tend to only mildly affect the medium-term trend of the geomagnetic field. Perhaps the best data assimilation approach in terms of forecasting could be one smartly combining 3D modelling of medium to long-term dynamo processes (along the lines described in Sect. 4.1), with 2D quasi-geostrophic modelling of short-term processes (along the lines described in Sect. 4.2).

One last outcome of the Hulot et al. (2010a) study worth mentioning is that it also implies that the timing of the next geomagnetic reversal is essentially unpredictable. As is indeed illustrated by Fig. 15, as soon as a perturbed solution has started diverging macroscopically from the reference solution, it behaves in a totally unrelated way. In particular, even if the reference solution was about to reverse, with already a fairly low axial dipole component, the perturbed solution may either postpone the reversal, or eventually decide not to reverse. Since it is well-known from examination of past reversals that these can hardly occur within less than a couple of thousand years when starting from dipole field value comparable to the present value (see e.g. Constable and Korte 2006; Hulot et al. 2010b), it is quite unavoidable that given the value of  $\tau_e = 30$  y expected for the geodynamo, predicting a reversal several millennia ahead of time would require a knowledge of the present state of the core way beyond our observational capacity.

## 5 Summary and Outlook

In this paper, we have motivated the development and implementation of data assimilation techniques for the purpose of geomagnetic data analysis. The ongoing era of magnetic observation of the Earth with satellites is a great and exciting incentive for investigating to what extent such techniques could be beneficial for improving both our understanding of core dynamics and our ability to model the core field. Of particular interest are the possibilities, on the one hand, to combine satellite data with observatory data to try and perform a reanalysis of historical field models over the past four hundred years or so, and, on the other hand, to produce better forecasts of the secular variation in the years to come.

We have succinctly introduced the basics of the algorithmic machinery in operational use in the atmospheric and oceanic communities in order to explain how to construct formally the relationship between a numerical model of core dynamics and geomagnetic observations. As we saw, the most critical points for its application to geomagnetism, compared to that in atmospheric or oceanic weather prediction, are

- that the observations directly access a much smaller fraction of the state vector,

– and that we still have to convince ourselves, in a trial-and-error fashion, that the various models that we use are adequate for this task.

Specific to the core problem is the remote, blurred and incomplete observation of its state. Accordingly, we lack a well-defined background state (the equivalent of a “climatological” mean), about which the dynamics of the secular variation is likely to take place, even though we have a fairly good idea of the large to medium length scales of the poloidal field at the top of the core over a 400 year period, and for the largest scales much longer back in time (e.g. Hulot et al. 2010b, and references therein). Also specific and important for geomagnetic data analysis is the need we are in to separate the various sources contributing to the field measured at a given location (in particular at satellite altitude). Our hope is that a better description of the core field by dynamical models could contribute to better recover it, in the same way similar approaches have already improved our understanding of the ionospheric and magnetospheric fields (e.g. Scherliess et al. 2006; Tsyganenko and Sitnov 2007).

The first results described in Sect. 4 indicate that, in the assimilation framework, surface measurements of  $B_r$  can provide some information and constraints about the structure of the field and the flow within the core. The propagation of the information (the innovation) from the core-mantle boundary to the bulk of the core is achieved either through the non-linear interactions between the dynamical actors (the various components of the state vector, which include the poloidal field), when operating with a three-dimensional model of the geodynamo, or by some a priori constraint imposed on the nature of the dynamics (under the quasi-geostrophic assumption, the invariance of the flow in the direction of rotation). There is room for improvement with respect to the way surface information is transferred to the bulk of the fluid: An appealing direction for future research in that area would be to resort to multivariate statistics and relate surface dynamical patterns with their roots, using empirical orthogonal functions. In oceanography, their use in conjunction with surficial observations leads to much better estimates of the state of the ocean, at least above the thermocline; see e.g. Penduff et al. (2002) for an illustration in the South Atlantic Ocean.

The issue of the climatological mean (the background state) for the core need also be looked at in detail. That mean could reflect the thermal control exerted on the core by the overlying mantle, which could thereby influence the long-term secular variation (e.g. Aubert et al. 2007). In addition, theoretical arguments favor a geodynamo operating close to a so-called Taylor state (Taylor 1963). It might then prove useful to seek an average core state  $\mathbf{x}^b$  satisfying Taylor’s constraint, which, following Sasaki (1970), could be enforced using either a weak or a strong formalism. For recent developments in that direction, the reader is referred to Livermore et al. (2009, 2010).

To conclude, let us emphasize that further understanding of the mechanisms controlling the short- and long-term secular variation and the internal structure and dynamics of the core could be gained by assimilating experimental results obtained with liquid metal analogs of the core. Such analogs are in use in several places around the globe (e.g. Cardin and Olson 2007, for a recent review): a container is filled with a liquid metal (sodium is today’s favorite working fluid), which is set in motion (most of the time by mechanical forcing), and can eventually support dynamo action in a turbulent environment (Monchaux et al. 2007). When well instrumented, liquid metal experiments have the advantage of providing a detailed mapping of the field at the surface of the container, possibly complemented by in-situ flow and field measurements (Nataf et al. 2006). Surface magnetic time series of the experimental secular variation can exhibit interesting features, which can be in turn interpreted as the signature of hydromagnetic waves (Schmitt et al. 2008). These time series have the advantage of lasting for several magnetic diffusion times (several hundreds of thousands of years when upscaled to the core). This is much more than the few centuries



of well-documented record of observations we have at hand for geomagnetic data assimilation practice. Even if the modest size of experimental analogs of the core ( $\approx 1$  m) creates a collapse of the various time scales over which the dynamical phenomena at work operate, it is almost certain that assimilating such experimental data could complement well the efforts currently led to better understand and model the physical principles governing the geomagnetic secular variation.

**Acknowledgements** We thank Ulrich Christensen for his thorough and stimulating review which greatly helped improve the manuscript. We are also grateful to Chris Finlay whose reading of the draft led to a much appreciated list of useful suggestions, and to Fabio Donadini for his assistance with the geomagia database. Alexandre Fournier, Dominique Jault, Elisabeth Canet and Nicolas Gillet have been supported by a grant from the French Agence Nationale de la Recherche, Research program VS-QG (grant number BLAN06-2.155316). Partial support also came from the program “observation de la Terre” of the French agency CNES, and from INSU, through the LEFE ASSIMILATION program. Weijia Kuang and Andrew Tangborn are funded by the NSF Collaborative Mathematical Geophysics (CMG) Program under the grant EAR-0327875, and by the NASA Earth’s Surface and Interior Program. The authors thank the International Space Science Institute and André Balogh for organizing the workshop on terrestrial magnetism held in Bern in March 2009. Alexandre Fournier also thanks gratefully Olivier Talagrand, Pierre Brasseur and Emmanuel Cosme for kindly and pedagogically distilling their knowledge of data assimilation over the past few years. Olivier Talagrand is especially thanked for explaining him, among other things, the subtleties of the “discrete of adjoint vs. adjoint of discrete” issue. Part of the figures were made using the following freely available softwares: the generic mapping tools (Wessel and Smith 1991), paraview ([www.paraview.org](http://www.paraview.org)), and the pstricks-add L<sup>A</sup>T<sub>E</sub>X package. This is IGP contribution 3033.

## References

- M.M. Alexandrescu, D. Gibert, J.L. Le Mouél, G. Hulot, G. Saracco, An estimate of average lower mantle conductivity by wavelet analysis of geomagnetic jerks. *J. Geophys. Res.* **104**(B8), 17735–17745 (1999). doi:[10.1029/1999JB900135](https://doi.org/10.1029/1999JB900135)
- H. Amit, J. Aubert, G. Hulot, P. Olson, A simple model for mantle-driven flow at the top of Earth’s core. *Earth Planets Space* **60**, 845–854 (2008)
- J. Aubert, H. Amit, G. Hulot, Detecting thermal boundary control in surface flows from numerical dynamos. *Phys. Earth Planet. Inter.* **160**(2), 143–156 (2007). doi:[10.1016/j.pepi.2006.11.003](https://doi.org/10.1016/j.pepi.2006.11.003)
- J. Aubert, H. Amit, G. Hulot, P. Olson, Thermochemical flows couple the Earth’s inner core growth to mantle heterogeneity. *Nature* **454**, 758–761 (2008). doi:[10.1038/nature07109](https://doi.org/10.1038/nature07109)
- G.E. Backus, Kinematics of geomagnetic secular variation in a perfectly conducting core. *Philos. Trans. R. Soc. Lond. Ser. A Math. Phys. Sci.* **263**(1141), 239–266 (1968)
- G.E. Backus, Application of mantle filter theory to the magnetic jerk of 1969. *Geophys. J. R. Astron. Soc.* **74**(3), 713–746 (1983)
- G. Backus, R. Parker, C. Constable, *Foundations of Geomagnetism* (Cambridge University Press, Cambridge, 1996)
- C.D. Beggan, K.A. Whaler, Forecasting change of the magnetic field using core surface flows and ensemble Kalman filtering. *Geophys. Res. Lett.* **36**, L18303 (2009). doi:[10.1029/2009GL039927](https://doi.org/10.1029/2009GL039927)
- A. Bennett, *Inverse Modeling of the Ocean and Atmosphere* (Cambridge University Press, Cambridge, 2002)
- P. Berghthorsson, B. Döös, Numerical weather map analysis. *Tellus* **7**(3), 329–340 (1955)
- J. Bloxham, D. Gubbins, A. Jackson, Geomagnetic secular variation. *Philos. Trans. R. Soc. Lond. Ser. A Math. Phys. Sci.*, 415–502 (1989)
- J. Bloxham, S. Zatman, M. Dumberry, The origin of geomagnetic jerks. *Nature* **420**(6911), 65–68 (2002). doi:[10.1038/nature01134](https://doi.org/10.1038/nature01134)
- S.I. Braginsky, Torsional magnetohydrodynamic vibrations of the earth’s core and variations in day length. *Geomagnet. Aeron.* **10**, 1–8 (1970)
- S.I. Braginsky, Short period geomagnetic variations. *Geophys. Astrophys. Fluid Dyn.* **30**, 1–78 (1984)
- P. Brasseur, Ocean data assimilation using sequential methods based on the Kalman filter, in *Ocean Weather Forecasting: An Integrated View of Oceanography*, ed. by E. Chassignet, J. Verron. (Springer, Berlin, 2006), pp. 271–316
- M. Buehner, Inter-comparison of 4D-Var and EnKF systems for operational deterministic numerical weather prediction, in *WWRP/THORPEX Workshop on 4D-VAR and Ensemble Kalman Filter Inter-comparisons*, Buenos Aires, Argentina, 2008
- B. Buffett, J. Mound, A. Jackson, Inversion of torsional oscillations for the structure and dynamics of Earth’s core. *Geophys. J. Int.* **177**(3), 878–890 (2009). doi:[10.1111/j.1365-246X.2009.04129.x](https://doi.org/10.1111/j.1365-246X.2009.04129.x)



- H.P. Bunge, C. Hagelberg, B. Travis, Mantle circulation models with variational data assimilation: inferring past mantle flow and structure from plate motion histories and seismic tomography. *Geophys. J. Int.* **152**(2), 280–301 (2003). doi:[10.1046/j.1365-246X.2003.01823.x](https://doi.org/10.1046/j.1365-246X.2003.01823.x)
- E. Canet, A. Fournier, D. Jault, Forward and adjoint quasi-geostrophic models of the geomagnetic secular variation. *J. Geophys. Res.* **114**, B11101 (2009). doi:[10.1029/2008JB006189](https://doi.org/10.1029/2008JB006189)
- P. Cardin, P. Olson, Experiments on core dynamics, in *Core Dynamics*, ed. by P. Olson, G. Schubert. Treatise on Geophysics, vol. 8 (Elsevier, Amsterdam, 2007), pp. 319–343, Chap. 11
- J.G. Charney, R. Fjortoft, J. Von Neumann, Numerical integration of the barotropic vorticity equation. *Tellus* **2**(4), 237–254 (1950)
- E. Chassignet, J. Verron, *Ocean Weather Forecasting: An Integrated View of Oceanography* (Springer, Berlin, 2006)
- U.R. Christensen, J. Aubert, Scaling properties of convection-driven dynamos in rotating spherical shells and application to planetary magnetic fields. *Geophys. J. Int.* **140**, 97–114 (2006). doi:[10.1111/j.1365-246X.2006.03009.x](https://doi.org/10.1111/j.1365-246X.2006.03009.x)
- U.R. Christensen, A. Tilgner, Power requirement of the geodynamo from ohmic losses in numerical and laboratory dynamos. *Nature* **429**(6988), 169–171 (2004). doi:[10.1038/nature02508](https://doi.org/10.1038/nature02508)
- U.R. Christensen, J. Wicht, Numerical dynamo simulations, in *Core Dynamics*, ed. by P. Olson, G. Schubert. Treatise on Geophysics, vol. 8 (Elsevier, Oxford, 2007), pp. 245–282, Chap. 8
- U.R. Christensen, V. Holzwarth, A. Reiners, Energy flux determines magnetic field strength of planets and stars. *Nature* **457**(7226), 167–169 (2009). doi:[10.1038/nature07626](https://doi.org/10.1038/nature07626)
- U.R. Christensen, J. Aubert, G. Hulot, Conditions for Earth-like geodynamo models. *Earth Planet. Sci. Lett.* (2010). doi:[10.1016/j.epsl.2010.06.009](https://doi.org/10.1016/j.epsl.2010.06.009)
- A. Chulliat, N. Olsen, Observation of magnetic diffusion in the Earth’s core from Magsat, Oersted and CHAMP data. *J. Geophys. Res.* **115**, B05105 (2010). doi:[10.1029/2009JB006994](https://doi.org/10.1029/2009JB006994)
- A. Chulliat, G. Hulot, L.R. Newitt, Magnetic flux expulsion from the core as a possible cause of the unusually large acceleration of the north magnetic pole during the 1990s. *J. Geophys. Res.* **115**, B07101 (2010). doi:[10.1029/2009JB007143](https://doi.org/10.1029/2009JB007143)
- S. Cohn, N. Sivakumaran, R. Todling, A fixed-lag Kalman smoother for retrospective data assimilation. *Mon. Weather Rev.* **122**(12), 2838–2867 (1994). doi:[10.1175/1520-0493\(1994\)122<2838:AFLKSF>2.0.CO;2](https://doi.org/10.1175/1520-0493(1994)122<2838:AFLKSF>2.0.CO;2)
- C. Constable, M. Korte, Is Earth’s magnetic field reversing? *Earth Planet. Sci. Lett.* **246**(1–2), 1–16 (2006). doi:[10.1016/j.epsl.2006.03.038](https://doi.org/10.1016/j.epsl.2006.03.038)
- E. Cosme, J.M. Brankart, J. Verron, P. Brasseur, M. Krysta, Implementation of a reduced-rank, square-root smoother for high resolution ocean data assimilation. *Ocean Model.* **33**(1–2), 87–100 (2010). doi:[10.1016/j.ocemod.2009.12.004](https://doi.org/10.1016/j.ocemod.2009.12.004)
- P. Courtier, Variational methods. *J. Meteorol. Soc. Jpn.* **75**(1B), 211–218 (1997)
- P. Courtier, O. Talagrand, Variational assimilation of meteorological observations with the adjoint vorticity equation. II: Numerical results. *Q. J. R. Meteorol. Soc.* **113**(478), 1329–1347 (1987). doi:[10.1002/gj.49711347813](https://doi.org/10.1002/gj.49711347813)
- D. Dee, A. Da Silva, Data assimilation in the presence of forecast bias. *Q. J. R. Meteorol. Soc.* **124**(545), 269–295 (1998)
- F. Donadini, M. Korte, C. Constable, Geomagnetic field for 0–3 ka: 1. New data sets for global modeling. *Geochem. Geophys. Geosyst.* **10**, Q06007 (2009). doi:[10.1029/2008GC002295](https://doi.org/10.1029/2008GC002295)
- G.D. Egbert, A.F. Bennett, M.G.G. Foreman, TOPEX/POSEIDON tides estimated using a global inverse model. *J. Geophys. Res.* **99**(C12), 24821–24852 (1994). doi:[10.1029/94JC01894](https://doi.org/10.1029/94JC01894)
- A. Eliassen, Provisional report on calculation of spatial covariance and autocorrelation of the pressure field. Institute of Weather and Climate Research, Academy of Sciences, Oslo, Report 5 (1954)
- G. Evensen, Sequential data assimilation with a nonlinear quasi-geostrophic model using Monte Carlo methods to forecast error statistics. *J. Geophys. Res.* **99**(C5), 10143–10162 (1994). doi:[10.1029/94JC00572](https://doi.org/10.1029/94JC00572)
- G. Evensen, *Data Assimilation: The Ensemble Kalman Filter*, 2nd edn. (Springer, Berlin, 2009). doi:[10.1007/978-3-642-03711-5](https://doi.org/10.1007/978-3-642-03711-5)
- C. Eymin, G. Hulot, On core surface flows inferred from satellite magnetic data. *Phys. Earth Planet. Inter.* **152**, 200–220 (2005). doi:[10.1016/j.pepi.2005.06.009](https://doi.org/10.1016/j.pepi.2005.06.009)
- A. Fichtner, H.P. Bunge, H. Igel, The adjoint method in seismology I. Theory. *Phys. Earth Planet. Inter.* **157**(1–2), 86–104 (2006). doi:[10.1016/j.pepi.2006.03.016](https://doi.org/10.1016/j.pepi.2006.03.016)
- C.C. Finlay, Historical variation of the geomagnetic axial dipole. *Phys. Earth Planet. Inter.* **170**(1–2), 1–14 (2008). doi:[10.1016/j.pepi.2008.06.029](https://doi.org/10.1016/j.pepi.2008.06.029)
- C.C. Finlay, A. Jackson, Equatorially dominated magnetic field change at the surface of earth’s core. *Science* **300**(5628), 2084–2086 (2003). doi:[10.1126/science.1083324](https://doi.org/10.1126/science.1083324)
- C.C. Finlay, M. Dumberry, A. Chulliat, A. Pais, Short timescale dynamics: Theory and observations. *Space Sci. Rev.* (2010, in revision)

- A. Fournier, C. Eymin, T. Alboussière, A case for variational geomagnetic data assimilation: insights from a one-dimensional, nonlinear, and sparsely observed MHD system. *Nonlinear Process. Geophys.* **14**, 163–180 (2007)
- E. Friis-Christensen, H. Lühr, G. Hulot, Swarm: A constellation to study the Earth's magnetic field. *Earth Planets Space* **58**, 351–358 (2006)
- L.S. Gandin, *Objective Analysis of Meteorological Fields (Objektivnyi Analiz Meteorologicheskikh Polei)* (Gidrometeor. Izd.i, Leningrad, 1963) (in Russian). English translation by Israel program for scientific translations, Jerusalem, 1965
- G. Gaspari, S.E. Cohn, Construction of correlation functions in two and three dimensions. *Q. J. R. Meteorol. Soc.* **125**(554), 723–757 (1999). doi:[10.1002/qj.49712555417](https://doi.org/10.1002/qj.49712555417)
- A. Genevey, Y. Gallet, C. Constable, M. Korte, G. Hulot, ArcheoInt: An upgraded compilation of geomagnetic field intensity data for the past ten millennia and its application to the recovery of the past dipole moment. *Geochem. Geophys. Geosyst.* **9**(4), Q04038 (2008). doi:[10.1029/2007GC001881](https://doi.org/10.1029/2007GC001881)
- A. Genevey, Y. Gallet, J. Rosen, M. Le Goff, Evidence for rapid geomagnetic field intensity variations in Western Europe over the past 800 years from new French archeointensity data. *Earth Planet. Sci. Lett.*, 132–143 (2009). doi:[10.1016/j.epsl.2009.04.024](https://doi.org/10.1016/j.epsl.2009.04.024)
- M. Ghil, P. Malanotte-Rizzoli, Data assimilation in meteorology and oceanography. *Adv. Geophys.* **33**, 141–266 (1991)
- R. Giering, T. Kaminski, Recipes for adjoint code construction. *ACM Trans. Math. Softw.* **24**(4), 437–474 (1998)
- N. Gillet, D. Brito, D. Jault, H.C. Nataf, Experimental and numerical studies of convection in a rapidly rotating spherical shell. *J. Fluid Mech.* **580**, 83–121 (2007). doi:[10.1017/S0022112007005265](https://doi.org/10.1017/S0022112007005265)
- N. Gillet, A. Pais, D. Jault, Ensemble inversion of time-dependent core flow models. *Geochem. Geophys. Geosyst.* **10**, Q06004 (2009). doi:[10.1029/2008GC002290](https://doi.org/10.1029/2008GC002290)
- N. Gillet, D. Jault, E. Canet, A. Fournier, Fast torsional waves and strong magnetic field within the Earth's core. *Nature* **465**, 74–77 (2010a). doi:[10.1038/nature09010](https://doi.org/10.1038/nature09010)
- N. Gillet, V. Lesur, N. Olsen, Geomagnetic core field secular variation models. *Space Sci. Rev.* (2010b, in press). doi:[10.1007/s11214-009-9586-6](https://doi.org/10.1007/s11214-009-9586-6)
- G.A. Glatzmaier, Numerical simulations of stellar convective dynamos. I—The model and method. *J. Comput. Phys.* **55**(3), 461–484 (1984). doi:[10.1016/0021-9991\(84\)90033-0](https://doi.org/10.1016/0021-9991(84)90033-0)
- G.A. Glatzmaier, P.H. Roberts, A three-dimensional self-consistent computer simulation of a geomagnetic reversal. *Nature* **377**, 203–209 (1995). doi:[10.1038/377203a0](https://doi.org/10.1038/377203a0)
- R.S. Gross, I. Fukumori, D. Menemenlis, P. Gegout, Atmospheric and oceanic excitation of length-of-day variations during 1980–2000. *J. Geophys. Res.* **109**, B01406 (2004). doi:[10.1029/2003JB002432](https://doi.org/10.1029/2003JB002432)
- D. Gubbins, A formalism for the inversion of geomagnetic data for core motions with diffusion. *Phys. Earth Planet. Inter.* **98**(3), 193–206 (1996). doi:[10.1016/S0031-9201\(96\)03187-1](https://doi.org/10.1016/S0031-9201(96)03187-1)
- D. Gubbins, N. Roberts, Use of the frozen flux approximation in the interpretation of archeomagnetic and palaeomagnetic data. *Geophys. J. R. Astron. Soc.* **73**(3), 675–687 (1983). doi:[10.1111/j.1365-246X.1983.tb03339.x](https://doi.org/10.1111/j.1365-246X.1983.tb03339.x)
- D. Gubbins, P.H. Roberts, Magnetohydrodynamics of the Earth's core, in *Geomagnetism*, vol. 2, ed. by J.A. Jacobs (Academic Press, London, 1987)
- D. Gubbins, A.L. Jones, C.C. Finlay, Fall in Earth's magnetic field is erratic. *Science* **312**(5775), 900–902 (2006). doi:[10.1126/science.1124855](https://doi.org/10.1126/science.1124855)
- N. Gustafsson, Discussion on '4D-Var or EnKF?'. *Tellus* **59A**(5), 774–777 (2007). doi:[10.1111/j.1600-0870.2007.00262.x](https://doi.org/10.1111/j.1600-0870.2007.00262.x)
- J.R. Heitzler, The future of the South Atlantic anomaly and implications for radiation damage in space. *J. Atmos. Sol.-Terr. Phys.* **64**(16), 1701–1708 (2002). doi:[10.1016/S1364-6826\(02\)00120-7](https://doi.org/10.1016/S1364-6826(02)00120-7)
- H. Hersbach, Application of the adjoint of the WAM model to inverse wave modeling. *J. Geophys. Res.* **103**(C 5), 10469–10487 (1998). doi:[10.1029/97JC03554](https://doi.org/10.1029/97JC03554)
- R. Hide, Free hydromagnetic oscillations of the Earth's core and the theory of the geomagnetic secular variation. *Philos. Trans. R. Soc. Lond. Ser. A Math. Phys. Sci.* **259**, 615–647 (1966)
- R. Holme, Large-scale flow in the core, in *Core Dynamics*, ed. by P. Olson, G. Schubert. Treatise on Geophysics, vol. 8 (Elsevier, Amsterdam, 2007), pp. 107–130, Chap. 4
- L. Hongre, G. Hulot, A. Khokhlov, An analysis of the geomagnetic field over the past 2000 years. *Phys. Earth Planet. Inter.* **106**(3), 311–335 (1998). doi:[10.1016/S0031-9201\(97\)00115-5](https://doi.org/10.1016/S0031-9201(97)00115-5)
- G. Hulot, J.L. Le Mouél, A statistical approach to the Earth's main magnetic field. *Phys. Earth Planet. Inter.* **82**(3), 167–183 (1994). doi:[10.1016/0031-9201\(94\)90070-1](https://doi.org/10.1016/0031-9201(94)90070-1)
- G. Hulot, M. Le Huy, J.L. Le Mouél, Secousses (jerks) de la variation séculaire et mouvements dans le noyau terrestre. *C. R. Acad. Sci. Sér. 2, Méc. Phys. Chim. Sci. Univers Sci. Terre* **317**(3), 333–341 (1993)
- G. Hulot, A. Khokhlov, J.L. Le Mouél, Uniqueness of mainly bipolar magnetic fields recovered from directional data. *Geophys. J. Int.* **129**(2), 347–354 (1997). doi:[10.1111/j.1365-246X.1997.tb01587.x](https://doi.org/10.1111/j.1365-246X.1997.tb01587.x)

- G. Hulot, C. Eymin, B. Langlais, M. Manda, N. Olsen, Small-scale structure of the geodynamo inferred from Oersted and Magsat satellite data. *Nature* **416**(6881), 620–623 (2002). doi:[10.1038/416620a](https://doi.org/10.1038/416620a)
- G. Hulot, T. Sabaka, N. Olsen, The present field, in *Geomagnetism*, ed. by M. Kono, G. Schubert. Treatise on Geophysics, vol. 5 (Elsevier, Amsterdam, 2007), Chap. 2
- G. Hulot, N. Olsen, E. Thebaud, K. Hemant, Crustal concealing of small-scale core-field secular variation. *Geophys. J. Int.* **177**(2), 361–366 (2009). doi:[10.1111/j.1365-246X.2009.04119.x](https://doi.org/10.1111/j.1365-246X.2009.04119.x)
- G. Hulot, F. Lhuillier, J. Aubert, Earth's dynamo limit of predictability. *Geophys. Res. Lett.* **37**, L06305 (2010a). doi:[10.1029/2009GL041869](https://doi.org/10.1029/2009GL041869)
- G. Hulot, C.C. Finlay, C.G. Constable, N. Olsen, M. Manda, The magnetic field of planet Earth. *Space Sci. Rev.* **152**(1–4), 159–222 (2010b). doi:[10.1007/s11214-010-9644-0](https://doi.org/10.1007/s11214-010-9644-0)
- K. Ide, P. Courtier, M. Ghil, A.C. Lorenc, Unified notation for data assimilation: Operational, sequential and variational. *J. Meteorol. Soc. Jpn.* **75**, 181–189 (1997)
- A. Jackson, The Earth's magnetic field at the core-mantle boundary. Ph.D. Thesis, Cambridge (1989)
- A. Jackson, Time-dependency of tangentially geostrophic core surface motions. *Phys. Earth Planet. Inter.* **103**, 293–311 (1997). doi:[10.1016/S0031-9201\(97\)00039-3](https://doi.org/10.1016/S0031-9201(97)00039-3)
- A. Jackson, C.C. Finlay, Geomagnetic secular variation and its application to the core, in *Geomagnetism*, ed. by P. Olson, G. Schubert. Treatise on Geophysics, vol. 5 (Elsevier, Amsterdam, 2007), pp. 148–193, Chap. 5
- A. Jackson, J. Bloxham, D. Gubbins, Time-dependent flow at the core surface and conservation of angular momentum in the coupled core–mantle system, in *Dynamics of Earth's Deep Interior and Earth Rotation*, ed. by J.L. Le Mouél, D.E. Smylie, T. Herring. (American Geophysical Union, Washington, 1993), pp. 97–107
- A. Jackson, A. Jonkers, M. Walker, Four centuries of geomagnetic secular variation from historical records. *Philos. Trans. R. Soc. Ser. A, Math. Phys. Eng. Sci.* **358**(1768), 957–990 (2000)
- D. Jault, Axial invariance of rapidly varying diffusionless motions in the Earth's core interior. *Phys. Earth Planet. Inter.* **166**(1–2), 67–76 (2008). doi:[10.1016/j.pepi.2007.11.001](https://doi.org/10.1016/j.pepi.2007.11.001)
- D. Jault, C. Gire, J.L. Le Mouél, Westward drift, core motions and exchanges of angular momentum between core and mantle. *Nature* **333**(6171), 353–356 (1988). doi:[10.1038/333353a0](https://doi.org/10.1038/333353a0)
- C. Jones, N. Weiss, F. Cattaneo, Nonlinear dynamos: a complex generalization of the Lorenz equations. *Physica D* **14**, 161–176 (1985). doi:[10.1016/0167-2789\(85\)90176-9](https://doi.org/10.1016/0167-2789(85)90176-9)
- A. Kageyama, T. Sato, Generation mechanism of a dipole field by a magnetohydrodynamic dynamo. *Phys. Rev. E* **55**(4), 4617–4626 (1997). doi:[10.1103/PhysRevE.55.4617](https://doi.org/10.1103/PhysRevE.55.4617)
- E. Kalnay, *Atmospheric Modeling, Data Assimilation, and Predictability* (Cambridge University Press, Cambridge, 2003)
- E. Kalnay, M. Kanamitsu, R. Kistler, W. Collins, D. Deaven, L. Gandin, M. Iredell, S. Saha, G. White, J. Woollen et al., The NCEP/NCAR 40-year reanalysis project. *Bull. Am. Meteorol. Soc.* **77**(3), 437–471 (1996). doi:[10.1175/1520-0477\(1996\)077<0437:TNRYRP>2.0.CO;2](https://doi.org/10.1175/1520-0477(1996)077<0437:TNRYRP>2.0.CO;2)
- E. Kalnay, H. Li, T. Miyoshi, S. Yang, J. Ballabrera-Poy, 4-D-Var or ensemble Kalman filter? *Tellus* **59A**(5), 758–773 (2007a). doi:[10.1111/j.1600-0870.2007.00261.x](https://doi.org/10.1111/j.1600-0870.2007.00261.x)
- E. Kalnay, H. Li, T. Miyoshi, S. Yang, J. Ballabrera-Poy, Response to the discussion on “4D-Var or EnKF?” by Nils Gustafsson. *Tellus* **59A**(5), 778–780 (2007b). doi:[10.1111/j.1600-0870.2007.00263.x](https://doi.org/10.1111/j.1600-0870.2007.00263.x)
- A. Kelbert, G. Egbert, A. Schultz, Non-linear conjugate gradient inversion for global EM induction: resolution studies. *Geophys. J. Int.* **173**(2), 365–381 (2008). doi:[10.1111/j.1365-246X.2008.03717.x](https://doi.org/10.1111/j.1365-246X.2008.03717.x)
- K. Korhonen, F. Donadini, P. Riisager, L.J. Pesonen, GEOMAGIA50: An archeointensity database with PHP and MySQL. *Geochem. Geophys. Geosyst.* **9**, Q04029 (2008). doi:[10.1029/2007GC001893](https://doi.org/10.1029/2007GC001893)
- M. Korte, C.G. Constable, Continuous geomagnetic field models for the past 7 millennia: 2. CALS7K. *Geochem. Geophys. Geosyst.* **6**(2), Q02H16 (2005). doi:[10.1029/2004GC000801](https://doi.org/10.1029/2004GC000801)
- M. Korte, F. Donadini, C.G. Constable, Geomagnetic field for 0–3 ka: 2. A new series of time-varying global models. *Geochem. Geophys. Geosyst.* **10**, Q06008 (2009). doi:[10.1029/2008GC002297](https://doi.org/10.1029/2008GC002297)
- W. Kuang, J. Bloxham, An Earth-like numerical dynamo model. *Nature* **389**(6649), 371–374 (1997). doi:[10.1038/38712](https://doi.org/10.1038/38712)
- W. Kuang, A. Tangborn, W. Jiang, D. Liu, Z. Sun, J. Bloxham, Z. Wei, MoSST-DAS: the first generation geomagnetic data assimilation framework. *Commun. Comput. Phys.* **3**, 85–108 (2008)
- W. Kuang, A. Tangborn, Z. Wei, T. Sabaka, Constraining a numerical geodynamo model with 100-years of geomagnetic observations. *Geophys. J. Int.* **179**(3), 1458–1468 (2009). doi:[10.1111/j.1365-246X.2009.04376.x](https://doi.org/10.1111/j.1365-246X.2009.04376.x)
- W. Kuang, Z. Wei, R. Holme, A. Tangborn, Prediction of geomagnetic field with data assimilation: a candidate secular variation model for IGRF-11. *Earth Planets Space* (2010, accepted)
- A. Kushinov, J. Velínský, P. Tarits, A. Semenov, O. Pankratov, L. Tøffner-Clausen, Z. Martinec, N. Olsen, T.J. Sabaka, A. Jackson, Level 2 products and performances for mantle studies with Swarm. ESA Technical Report (2010)

- F.X. Le Dimet, O. Talagrand, Variational algorithms for analysis and assimilation of meteorological observations: Theoretical aspects. *Tellus* **38**(2), 97–110 (1986)
- B. Lehnert, Magnetohydrodynamic waves under the action of the Coriolis force. *Astrophys. J.* **119**, 647–654 (1954). doi:[10.1086/145869](https://doi.org/10.1086/145869)
- V. Lesur, I. Wardinski, Comment on “Can core-surface flow models be used to improve the forecast of the Earth’s main magnetic field?” by Stefan Maus, Luis Silva, and Gauthier Hulot. *J. Geophys. Res.* **114**, B04104 (2009). doi:[10.1029/2008JB006188](https://doi.org/10.1029/2008JB006188)
- V. Lesur, I. Wardinski, M. Rother, M. Manda, GRIMM: the GFZ reference internal magnetic model based on vector satellite and observatory data. *Geophys. J. Int.* **173**(2), 382–394 (2008). doi:[10.1111/j.1365-246X.2008.03724.x](https://doi.org/10.1111/j.1365-246X.2008.03724.x)
- V. Lesur, I. Wardinski, S. Asari, B. Minchev, M. Manda, Modelling the Earth’s core magnetic field under flow constraints. *Earth Planets Space* (2010). doi:[10.5047/eps.2010.02.010](https://doi.org/10.5047/eps.2010.02.010)
- L. Liu, M. Gurnis, Simultaneous inversion of mantle properties and initial conditions using an adjoint of mantle convection. *J. Geophys. Res.* **113**, B8405 (2008). doi:[10.1029/2008JB005594](https://doi.org/10.1029/2008JB005594)
- D. Liu, A. Tangborn, W. Kuang, Observing system simulation experiments in geomagnetic data assimilation. *J. Geophys. Res.* **112**, B8 (2007). doi:[10.1029/2006JB004691](https://doi.org/10.1029/2006JB004691)
- L. Liu, S. Spasojevic, M. Gurnis, Reconstructing Farallon plate subduction beneath North America back to the late cretaceous. *Science* **322**(5903), 934–938 (2008). doi:[10.1126/science.1162921](https://doi.org/10.1126/science.1162921)
- P.W. Livermore, G.R. Ierley, A. Jackson, The construction of exact Taylor states. I: The full sphere. *Geophys. J. Int.* **179**(2), 923–928 (2009). doi:[10.1111/j.1365-246X.2009.04340.x](https://doi.org/10.1111/j.1365-246X.2009.04340.x)
- P.W. Livermore, G.R. Ierley, A. Jackson, The construction of exact Taylor states. II: The influence of an inner core. *Phys. Earth Planet. Inter.* **178**, 16–26 (2010). doi:[10.1016/j.pepi.2009.07.015](https://doi.org/10.1016/j.pepi.2009.07.015)
- A.C. Lorenc, Analysis methods for numerical weather prediction. *Q. J. R. Meteorol. Soc.* **112**(474), 1177–1194 (1986). doi:[10.1002/qj.49711247414](https://doi.org/10.1002/qj.49711247414)
- E.N. Lorenz, Deterministic nonperiodic flow. *J. Atmos. Sci.* **20**(2), 130–141 (1963)
- S. Maus, S. Macmillan, T. Chernova, S. Choi, D. Dater, V. Golovkov, V. Lesur, F. Lowes, H. Lühr, W. Mai, S. McLean, N. Olsen, M. Rother, T. Sabaka, A. Thomson, T. Zvereva, The 10th-generation international geomagnetic reference field. *Geophys. J. Int.* **161**, 561–565 (2005). doi:[10.1111/j.1365-246X.2005.02641.x](https://doi.org/10.1111/j.1365-246X.2005.02641.x)
- S. Maus, L. Silva, G. Hulot, Can core-surface flow models be used to improve the forecast of the Earth’s main magnetic field? *J. Geophys. Res.* **113**, B08102 (2008). doi:[10.1029/2007JB005199](https://doi.org/10.1029/2007JB005199)
- S. Maus, L. Silva, G. Hulot, Reply to comment by V. Lesur et al. on “Can core-surface flow models be used to improve the forecast of the Earth’s main magnetic field?”. *J. Geophys. Res.* **114**, B04105 (2009). doi:[10.1029/2008JB006242](https://doi.org/10.1029/2008JB006242)
- H. Meyers, W.M. Davis, A profile of the geomagnetic model users and abusers. *J. Geomagn. Geoelectr.* **42**(9), 1079–1085 (1990)
- R.N. Miller, M. Ghil, F. Gauthiez, Advanced data assimilation in strongly nonlinear dynamical systems. *J. Atmos. Sci.* **51**(8), 1037–1056 (1994). doi:[10.1175/1520-0469\(1994\)051<1037:ADAISN>2.0.CO;2](https://doi.org/10.1175/1520-0469(1994)051<1037:ADAISN>2.0.CO;2)
- R. Monchaux, M. Berhanu, M. Bourgoin, M. Moulin, P. Odier, J.F. Pinton, R. Volk, S. Fauve, N. Mordant, F. Pétrélis, et al., Generation of a magnetic field by dynamo action in a turbulent flow of liquid sodium. *Phys. Rev. Lett.* **98**(4), 044502 (2007). doi:[10.1103/PhysRevLett.98.044502](https://doi.org/10.1103/PhysRevLett.98.044502)
- H.C. Nataf, T. Alboussière, D. Brito, P. Cardin, N. Gagnière, D. Jault, J.P. Masson, D. Schmitt, Experimental study of super-rotation in a magnetostrophic spherical Couette flow. *Geophys. Astrophys. Fluid Dyn.* **100**, 281–298 (2006). doi:[10.1080/03091920600718426](https://doi.org/10.1080/03091920600718426)
- N. Olsen, M. Manda, Rapidly changing flows in the earth’s core. *Nat. Geosci.* **1**, 390–394 (2008). doi:[10.1038/ngeo203](https://doi.org/10.1038/ngeo203)
- N. Olsen, R. Holme, G. Hulot, T. Sabaka, T. Neubert, L. Tøffner-Clausen, F. Primdahl, J. Jørgensen, J. Léger, D. Barraclough, J. Bloxham, J. Cain, C. Constable, V. Golovkov, A. Jackson, P. Kotze, B. Langlais, S. Macmillan, M. Manda, J. Merayo, L. Newitt, M. Purucker, T. Risbo, M. Stampe, A. Thomson, C. Voorhies, Ørsted initial field model. *Geophys. Res. Lett.* **27**(22), 3607–3610 (2000). doi:[10.1029/2000GL011930](https://doi.org/10.1029/2000GL011930)
- N. Olsen, H. Lühr, T.J. Sabaka, M. Manda, M. Rother, L. Tøffner-Clausen, S. Choi, CHAOS-a model of the Earth’s magnetic field derived from CHAMP, Ørsted, and SAC-C magnetic satellite data. *Geophys. J. Int.* **166**(1), 67–75 (2006). doi:[10.1111/j.1365-246X.2006.02959.x](https://doi.org/10.1111/j.1365-246X.2006.02959.x)
- N. Olsen, M. Manda, T. Sabaka, L. Tøffner-Clausen, CHAOS-2—a geomagnetic field model derived from one decade of continuous satellite data. *Geophys. J. Int.* **179**(3), 1477–1487 (2009). doi:[10.1111/j.1365-246X.2009.04386.x](https://doi.org/10.1111/j.1365-246X.2009.04386.x)
- A. Pais, G. Hulot, Length of day decade variations, torsional oscillations and inner core superrotation: evidence from recovered core surface zonal flows. *Phys. Earth Planet. Inter.* **118**(3–4), 291–316 (2000). doi:[10.1016/S0031-9201\(99\)00161-2](https://doi.org/10.1016/S0031-9201(99)00161-2)

- T. Penduff, P. Brasseur, C. Testut, B. Barnier, J. Verron, A four-year eddy-permitting assimilation of sea-surface temperature and altimetric data in the South Atlantic Ocean. *J. Mar. Res.* **60**(6), 805–833 (2002). doi:[10.1357/002224002321505147](https://doi.org/10.1357/002224002321505147)
- K. Pinheiro, A. Jackson, Can a 1-D mantle electrical conductivity model generate magnetic jerk differential time delays? *Geophys. J. Int.* **173**(3), 781–792 (2008). doi:[10.1111/j.1365-246X.2008.03762.x](https://doi.org/10.1111/j.1365-246X.2008.03762.x)
- L.F. Richardson, *Weather Prediction by Numerical Process* (Cambridge University Press, Cambridge, 1922)
- P.H. Roberts, S. Scott, On analysis of the secular variation. *J. Geomagn. Geoelectr.* **17**(2), 137–151 (1965)
- T. Sabaka, N. Olsen, M. Purucker, Extending comprehensive models of the Earth's magnetic field with Ørsted and CHAMP data. *Geophys. J. Int.* **159**(2), 521–547 (2004). doi:[10.1111/j.1365-246X.2004.02421.x](https://doi.org/10.1111/j.1365-246X.2004.02421.x)
- A. Sakuraba, P.H. Roberts, Generation of a strong magnetic field using uniform heat flux at the surface of the core. *Nat. Geosci.* **2**, 802–805 (2009). doi:[10.1038/ngeo643](https://doi.org/10.1038/ngeo643)
- M. Sambridge, P. Rickwood, N. Rawlinson, S. Sommacal, Automatic differentiation in geophysical inverse problems. *Geophys. J. Int.* **170**(1), 1–8 (2007). doi:[10.1111/j.1365-246X.2007.03400.x](https://doi.org/10.1111/j.1365-246X.2007.03400.x)
- Y. Sasaki, Some basic formalisms in numerical variational analysis. *Mon. Weather Rev.* **98**(12), 875–883 (1970). doi:[10.1175/1520-0493\(1970\)098<0875:SBFINV>2.3.CO;2](https://doi.org/10.1175/1520-0493(1970)098<0875:SBFINV>2.3.CO;2)
- L. Scherliess, R.W. Schunk, J.J. Sojka, D.C. Thompson, L. Zhu, Utah State University Global Assimilation of Ionospheric Measurements Gauss-Markov Kalman filter model of the ionosphere: Model description and validation. *J. Geophys. Res.* **111**, A11315 (2006). doi:[10.1029/2006JA011712](https://doi.org/10.1029/2006JA011712)
- D. Schmitt, T. Alboussière, D. Brito, P. Cardin, N. Gagnière, D. Jault, H.C. Nataf, Rotating spherical Couette flow in a dipolar magnetic field: experimental study of magneto-inertial waves. *J. Fluid Mech.* **604**, 175–197 (2008). doi:[10.1017/S0022112008001298](https://doi.org/10.1017/S0022112008001298)
- Z. Sun, A. Tangborn, W. Kuang, Data assimilation in a sparsely observed one-dimensional modeled MHD system. *Nonlinear Process. Geophys.* **14**(2), 181–192 (2007)
- F. Takahashi, M. Matsushima, Y. Honkura, Scale variability in convection-driven mhd dynamos at low Ekman number. *Phys. Earth Planet. Inter.* **167**, 168–178 (2008). doi:[10.1016/j.pepi.2008.03.005](https://doi.org/10.1016/j.pepi.2008.03.005)
- O. Talagrand, The use of adjoint equations in numerical modelling of the atmospheric circulation, in *Automatic Differentiation of Algorithms: Theory, Implementation, and Application*, ed. by A. Griewank, G.G. Corliss. (Society for Industrial and Applied Mathematics, Philadelphia, 1991), pp. 169–180
- O. Talagrand, Assimilation of observations, an introduction. *J. Meteorol. Soc. Jpn.* **75**(1B), 191–209 (1997)
- O. Talagrand, A posteriori validation of assimilation algorithms, in *Data Assimilation for the Earth System*, ed. by R. Swinbank, V. Shutyaev, W. Lahoz. (Kluwer Academic, Dordrecht, 2003), pp. 85–95
- O. Talagrand, P. Courtier, Variational assimilation of meteorological observations with the adjoint vorticity equation. I: Theory. *Q. J. R. Meteorol. Soc.* **113**(478), 1311–1328 (1987). doi:[10.1002/gj.49711347812](https://doi.org/10.1002/gj.49711347812)
- A. Tarantola, Inversion of seismic reflection data in the acoustic approximation. *Geophysics* **49**(8), 1259–1266 (1984). doi:[10.1190/1.1441754](https://doi.org/10.1190/1.1441754)
- A. Tarantola, Theoretical background for the inversion of seismic waveforms including elasticity and attenuation. *Pure Appl. Geophys.* **128**(1), 365–399 (1988). doi:[10.1007/BF01772605](https://doi.org/10.1007/BF01772605)
- J.B. Taylor, The magneto-hydrodynamics of a rotating fluid and the earth's dynamo problem. *Proc. R. Soc. Lond. Ser. A, Math. Phys. Sci.* **274**(1357), 274–283 (1963)
- E. Thébaud, A. Chulliat, S. Maus, G. Hulot, B. Langlais, A. Chambodut, M. Menvielle, IGRF candidate models at times of rapid changes in core field acceleration. *Earth Planets Space* (2010). doi:[10.5047/eps.2010.05.004](https://doi.org/10.5047/eps.2010.05.004)
- Y. Trémolet, Accounting for an imperfect model in 4D-Var. *Q. J. R. Meteorol. Soc.* **132**(621), 2483–2504 (2006). doi:[10.1256/qj.05.224](https://doi.org/10.1256/qj.05.224)
- J. Tromp, C. Tape, Q. Liu, Seismic tomography, adjoint methods, time reversal and banana-doughnut kernels. *Geophys. J. Int.* **160**(1), 195–216 (2005). doi:[10.1111/j.1365-246X.2004.02453.x](https://doi.org/10.1111/j.1365-246X.2004.02453.x)
- J. Tromp, D. Komatitsch, Q. Liu, Spectral-element and adjoint methods in seismology. *Commun. Comput. Phys.* **3**, 1–32 (2008)
- N.A. Tsyganenko, M.I. Sitnov, Magnetospheric configurations from a high-resolution data-based magnetic field model. *J. Geophys. Res.* **112**, A06225 (2007). doi:[10.1029/2007JA012260](https://doi.org/10.1029/2007JA012260)
- F. Uboldi, M. Kamachi, Time-space weak-constraint data assimilation for nonlinear models. *Tellus A* **52**(4), 412–421 (2000). doi:[10.1034/j.1600-0870.2000.00878.x](https://doi.org/10.1034/j.1600-0870.2000.00878.x)
- R. Waddington, D. Gubbins, N. Barber, Geomagnetic field analysis-V. Determining steady core-surface flows directly from geomagnetic observations. *Geophys. J. Int.* **122**(1), 326–350 (1995). doi:[10.1111/j.1365-246X.1995.tb03556.x](https://doi.org/10.1111/j.1365-246X.1995.tb03556.x)
- P. Wessel, W.H.F. Smith, Free software helps map and display data. *Trans. Am. Geophys. Union* **72**, 441–445 (1991). doi:[10.1029/90EO00319](https://doi.org/10.1029/90EO00319)
- K. Whaler, D. Gubbins, Spherical harmonic analysis of the geomagnetic field: an example of a linear inverse problem. *Geophys. J. R. Astron. Soc.* **65**(3), 645–693 (1981). doi:[10.1111/j.1365-246X.1981.tb04877.x](https://doi.org/10.1111/j.1365-246X.1981.tb04877.x)
- C. Wunsch, *Discrete Inverse and State Estimation Problems* (Cambridge University Press, Cambridge, 2006)